UNIVERSITÀ
DEGLI STUDI
FIRENZE

DOTTORATO DI RICERCA IN
SCIENZE CHIMICHE

CICLO XXIX

COORDINATORE Prof. PIERO BAGLIONI

FEASIBILITY OF FT-IR SPECTROSCOPY AS A SUPPORTING TOOL FOR RADIOCARBON DATING OF RESTORED SAMPLES

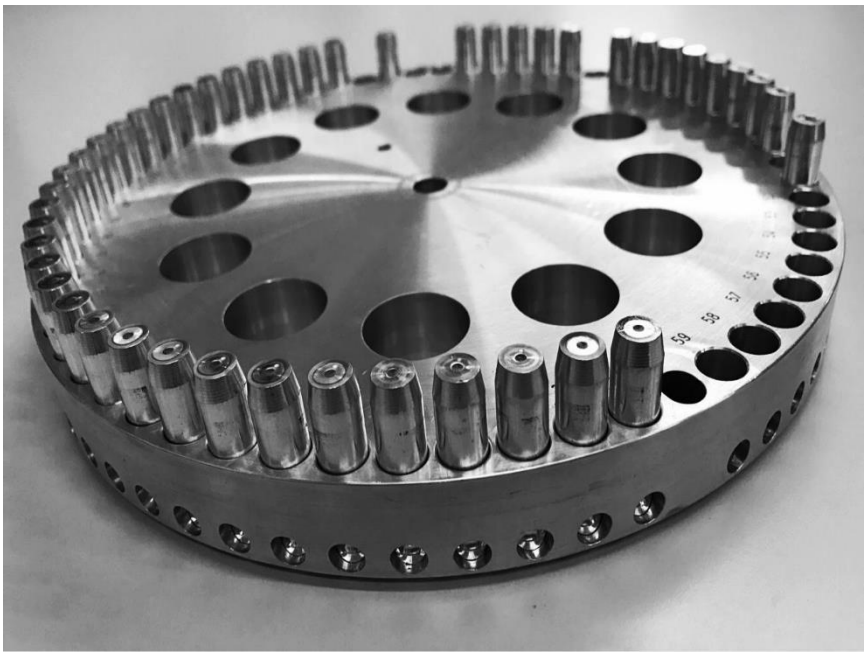

Dottorando
Dott.ssa Lucia Liccioli

Tutore
Prof. Pier Andrea Mandò

Co-Tutore
Dott.ssa Mariaelena Fedi

UNIVERSITÀ
DEGLI STUDI
FIRENZE

DOTTORATO DI RICERCA IN SCIENZE CHIMICHE

CICLO XXIX

COORDINATORE Prof. PIERO BAGLIONI

FEASIBILITY OF FT-IR SPECTROSCOPY AS A SUPPORTING TOOL FOR RADIOCARBON DATING OF RESTORED SAMPLES

Settore Scientifico Disciplinare CHIM/12

Dottorando
Dott. Lucia Liccioli

Tutore
Prof. Pier Andrea Mandò

Co-Tutore
Dott.ssa Mariaelena Fedi

Coordinatore
Prof. Piero Baglioni

Anni 2013/2016

Summary

Introduction

The research developed during my PhD has been performed principally at the LABEC laboratory (Laboratorio di Tecniche Nucleari per l'Ambiente e i Beni Culturali) of INFN-Florence (Istituto Nazionale di Fisica Nucleare) and University of Florence, where a 3 MV tandem accelerator is installed. One of the research lines of LABEC is dedicated to Accelerator Mass Spectrometry (AMS). This technique allows us to detect the relative abundance of rare isotopes, e.g. ^{14}C, which is at the base of one of the most important dating methods. Radiocarbon dating was developed by the American Nobel prize W.F. Libby. During the '40s and '50s of the 20th century, Libby studied the possibility to measure the relative abundances of the carbon isotopes. The measurement of the residual abundance of ^{14}C atoms (or its activity) allows dating organic samples as, e.g. charcoals, bones and textiles. Radiocarbon dating has given an essential contribution to several disciplines such as archaeology and art history, but also geology, paleoclimatology, atmospheric science and biomedicine.

My PhD activity concerned applications of radiocarbon to archaeology and Cultural Heritage. I have especially focused to all the phases involving the preparation and the pre-treatment of samples to be radiocarbon dated. In fact, one of the main assumptions of radiocarbon dating is considering the sample as a closed system once the exchanges with the environment are ceased (and this is typically coincides with

the death of the organism). The non-removal of possible exogenous carbon entails contaminations that cause measurements to be affected by systematic errors.

In particular, I worked on those samples that were characterised by either restoration or consolidation events. If the applied products are not removed during the pre-treatment phase, they can produce an apparent aging of the sample due to decrease of the radiocarbon concentration. Indeed, it is well known that since the 1960s, the products employed have been based on synthetic materials, rich in fossil carbon. Among the synthetic resins, Paraloid B72® is one of the most widespread products for restoration of many materials as wood, canvas and bones. The mechanical cleaning and the simple pre-treatment Acid-Base-Acid (ABA), usually applied to clean the samples to be dated from naturally occurring pollutants, are not sufficient to eliminate this kind of contamination. I have worked on a new procedure using chloroform ($CHCl_3$) as the key solvent.

The first step in the research activity has been checking the effectiveness of chloroform as a solvent for the removal of Paraloid B72. The second step has been testing the Fourier Transform Infrared Spectroscopy (FT-IR) technique as a supporting tool to answer to basic questions: whether estimate if Paraloid B72 is present on the sample to be dated is possible and whether we can discriminate if our sample pre-treatment has been successful in the removal the possible contaminants. FT-IR has been chosen thanks to its great sensitivity to detect the functional groups of organic molecules. In addition, FT-IR technique requires small samples to acquire a spectrum. This is definitely one of the key points when dealing with samples in the field of Cultural Heritage.

I principally focused on wood and bone samples. These materials were chosen because they represent very usual samples in radiocarbon dating. Wood is one of the most common materials in the Cultural Heritage field and bones are the typical findings in an archaeological context. Moreover, they can provide a lot of useful information to reconstruct historical events.

In the first chapter of this thesis, the basic principles of radiocarbon dating are described, in particular the attention is focused on the issue of contamination due to fossil carbon. In addition, some techniques to investigate the possible presence of organic contaminants are presented.

In the second chapter, the 3 MV Tandem accelerator installed at LABEC is explained presenting the AMS beam line with reference to radiocarbon measurements. Moreover, the standard sample preparation procedure for radiocarbon dating (pre-treatment, combustion and graphitization processes) that is necessary to obtain a graphite pellet to be measured by AMS is introduced.

In chapter three, the new chloroform-based procedure, to remove the contamination due to Paraloid B72, is shown with reference to case of wooden restored framework. Moreover, possible cross-contaminations due to the experimental setup are discussed.

In the fourth chapter, in order to better understand the effectiveness of the chloroform-based procedure, the pre-treatment is applied to wooden test samples contaminated on purpose. AMS measurements and FT-IR analyses are discussed.

In the last chapter, the chloroform-based procedure is applied on restored bones collected from the Anthropological Museum collection of University of Florence. These broken bones had been restored using Paraloid B72. AMS measurements and FT-IR analyses are discussed. Moreover, the chloroform-based procedure is applied to consolidated bone samples collected during an archaeological survey in the south of Cyprus.

1. Radiocarbon method

The possibility to measure the residual abundance of radiocarbon in a sample is surely the principal radiometric method to study the past and in particular to date organic findings. In order that the measured ^{14}C concentration be used for a correct dating, the sample must be considered as a closed system starting from the moment of death of the organism the sample is derived from. If this key point is not respected, the material might be contaminated by exogenous carbon that must be removed before the measurement of ^{14}C concentration. The possibility to perform some diagnostics before, during and after sample preparation to identify the possible contamination and to verify its complete removal is therefore very important.

1.1 Radiocarbon dating fundamentals

It is well known that carbon, one of the most common elements present on earth, has three natural isotopes: ^{12}C, ^{13}C and ^{14}C. The first two isotopes are stable and represent almost the whole carbon (indeed their concentrations in nature are 98.9% and 1.1%, respectively). The third is the only unstable natural carbon isotope and it represents a very small part (the ratio $^{14}C/^{12}C$ is about 1.2×10^{-12}).

If the nucleus of an atom is unstable, it can decay to a different state emitting radiation. This process is subjected to a probabilistic law; actually, it is impossible to predict when a nucleus will decay. Nevertheless, given a closed collection of unstable

nuclei, we can describe how the total number will change as time is passing by: it will decrease according to an exponential law. The ^{14}C nucleus decays via beta emission to the ground state of ^{14}N with a half-life $T_{1/2}$=5700±30 years [Kut2013], producing an electron and an uncharged particle (antineutrino $\bar{\nu}$):

$$^{14}C \rightarrow {}^{14}N + \beta^- + \bar{\nu} \qquad (1.1)$$

Radiocarbon is continuously formed in the upper atmosphere by the interaction of secondary products of cosmic rays, the thermal neutrons, with ^{14}N nuclei [Bow1990]. Once radiocarbon is produced, the ^{14}C combines with oxygen forming $^{14}CO_2$. The $^{14}CO_2$ from the atmosphere becomes part of the carbon cycle spreading out into the soil, the seas and the whole biosphere, at first through diffusion process and photosynthesis, and then thanks to food chain mechanisms. As we can consider the production rate of radiocarbon constant, there is a balance between the production and the decay and then there is a constant concentration of ^{14}C in the atmosphere[1]. Consequently, there is a dynamic equilibrium in all living organisms and the environment.

When an organism dies, we can consider it as a closed system because the exchanges with the external environment are interrupted. If there is no other mechanism of formation or uptake of carbon, the number of ^{12}C and ^{13}C atoms remain constant, while the number of ^{14}C decreases according to the radioactive decay law [Bow1990]. After a period t from the instant of death, the residual radiocarbon concentration $^{14}R(t)$ can be described as:

$$^{14}R_{(t)} = \frac{^{14}C}{C_{total}} \approx \frac{^{14}C}{^{12}C} = {}^{14}R_0 \cdot e^{-\frac{t}{\tau}} \qquad (1.2)$$

[1] Since the ^{14}C lifetime is short with respect to the age of Earth, we can consider that the secular equilibrium between the production and the decay has been reached.

In equation (1.2), ${}^{14}R_0$ is the radiocarbon concentration at the moment of death and τ is the ^{14}C mean lifetime. For each radioactive isotope, the mean lifetime is specific and it is related to the half-life ($T_{1/2}$) by the following expression:

$$\tau = \frac{T_{1/2}}{\ln 2} \tag{1.3}$$

If the mean lifetime τ is known and if it is possible to measure the number of the residual radioisotopes, we can determine how much time t has elapsed since the moment of death:

$$t = \tau \cdot \ln\left[\frac{{}^{14}R_0}{{}^{14}R_t}\right] \tag{1.4}$$

The estimated t in equation 1.4 is defined as the conventional radiocarbon age t_{RC} when τ is taken as the conventional mean lifetime of 8033 years, which is the so-called "Libby mean lifetime[2]". The radiocarbon age is also defined adopting the conventional value of 1.18×10^{-12} as the radiocarbon concentration in atmosphere in a reference year, i.e. 1950. This was chosen because, in the immediately following years, the radiocarbon concentration has increased very quickly due to nuclear weapons tests (see paragraph 1.2.2). The conventional radiocarbon age is expressed in years Before Present (years BP), where Present is 1950.

[2] Libby was the first to measure the radiocarbon decay rate, determining a half-life of 5568 years, the so-called "Libby half-life". The most recent measurements agree on the already mentioned estimate of about 5700 years.

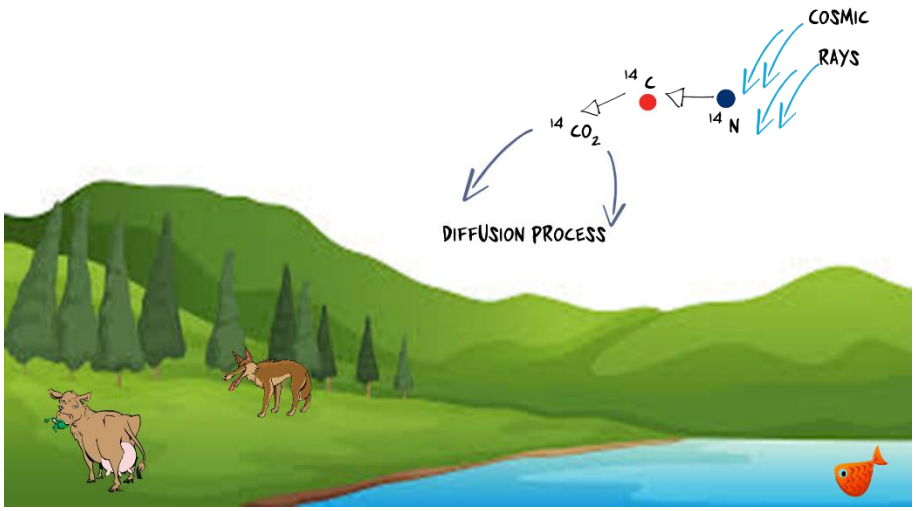

Figure 1.1 - Schematic representation of the carbon cycle and how ^{14}C enters into the biosphere.

Using radiocarbon, in principle, it is therefore possible to date all those materials that have been part of the biosphere as an animal (for example, bones, shells, wool, silk...) or something of vegetal origin (wood, charcoal, flax, cotton…). At present, considering the capabilities of the current measurement techniques, it is possible to date samples back to about 50000 years ago. In fact, in older samples, the residual number of ^{14}C atoms is too low to be detected.

1.2 Key assumptions in radiocarbon dating

Actually, the conventional radiocarbon age obtained using equation (1.4) does not correspond to the "real" age of the sample. Indeed, t_{RC}, besides being derived using conventional values for τ and R_0, is based on assumptions that are true only as a first approximation. They will be discussed in the following. In particular, the important hypothesis of the closed system will be discussed in paragraph 1.4.

1.2.1 Constancy of ^{14}C concentration in the atmosphere with respect to place

Equation (1.4) has a general value if we consider that radiocarbon concentration in the atmosphere does not depend on geographic factors, in particular latitude.

The Earth's geomagnetic field directly influences the production of radiocarbon in atmosphere because it is not homogeneous [see e.g. Bur2013]. The cosmic rays, from which thermal neutrons derive, are charged particles and therefore they are deflected in a magnetic field: the ^{14}C production rate is higher at the poles, where the field lines are steeper, compared to Equator (see Figure 1.2).

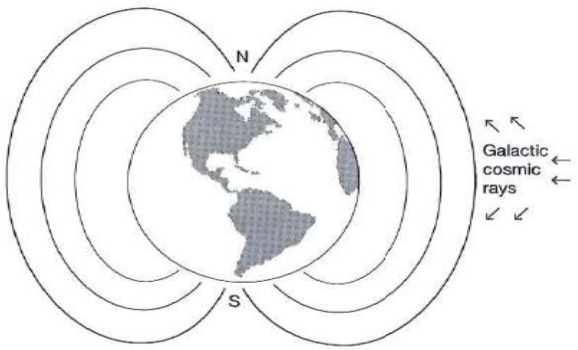

Figure 1.2 - Sketch of the geomagnetic field surrounding the Earth. The geomagnetic field deflects cosmic radiation more strongly at the Equator [Bur2013].

However, the atmospheric flows countinuously move the air masses. The periods, during which this mixing occurs, are very short compared to the radiocarbon decay time and so the higher production rate at the pole has a negligible effect on radiocarbon concentration. For this reason, the radiocarbon concentration in the whole atmosphere can be considered as homogeneous to a good approximation.

Nevertheless, slight differences in the atmospheric radiocarbon concentrations between the two emispheres are present. In the Southern emisphere the ^{14}C levels are typically registered as lower than those in the Northen emisphere [Hog2011]. The differences can be explained considering the bigger ocean surface present in the

Southern emisphere, acting as a stronger carbon reservoir. However, the differences in the ^{14}C concentration are very small and possibly require minor corrections (of the order of few years) [Hog2013].

In addition, on a local scale, short-term variations may be caused by volcanic eruptions that can induce changes in the atmospheric ^{14}C concentration. During these natural events, a big quantity of fossil carbon dioxide, basically with a very low content of ^{14}C, is introduced into the atmosphere. However, in these cases, the variation of radiocarbon concentration can be considered an effect just on a regional scale and it is strongly attenuated within a short time by the reservoir effect of the atmosphere itself.

1.2.2 Constancy of ^{14}C concentration in the atmosphere with respect to time

A discrepancy between samples of known ages and their measured radiocarbon ages has been already noticed since the early tests. This difference can be explained considering that radiocarbon concentration in the atmosphere (and consequently in the living organisms in equilibrium with the atmosphere) has not been truly constant in the past, with considerable variations. The reasons of these variations are both natural and anthropogenic.

-The natural causes

The atmospheric radiocarbon production is influenced by variations of the solar activity, which is responsible for most of the primary cosmic rays. The well known 11-years solar cycle does not however impact on the radiocarbon concentration, because the consequent changes of the production rate are balanced with the reservoir effect owing to their very short period compared to the ^{14}C mean lifetime. On the contrary, the solar cycle characterised by the longer period of about 200 years has an appreciable consequence on the radiocarbon concentration [Bur2013].

Not only is the geomagnetic field responsible for the highest prodution rate of ^{14}C at the poles with respect to the Equator, but it also influences the radiocarbon content

of atmosphere in different periods as a consequence of its variations in direction and magnitude. These changes occur during a long period, which is comparable with radiocarbon mean lifetime. The ^{14}C concentration present in atmosphere and the geomagnetic field strenght can be described as inversely related [Bur2013].

-The anthropogenic causes

In the last two-three centuries, the atmospheric ^{14}C concentration has been principally influenced by two different effects due to the human activities.

During the Industrial Revolution, a widespread use of fossil fuels began because of the employment of the new steam machineries. A large amount of carbon dioxide was released in atmosphere causing a significant impact on ^{14}C; in fact, this kind of CO_2 was originated from coal combustion and for this reason was devoid of radiocarbon. The combustion of such fuels has continuously increased since the late eighteenth century, decreasing the $^{14}C/^{12}C$ isotopic ratio in atmosphere and consequently in the biosphere. This dilution phenomenon is known in the literature as "Suess effect" because it was first described by Hans Suess in 1953 [Sue1955, Lev1989].

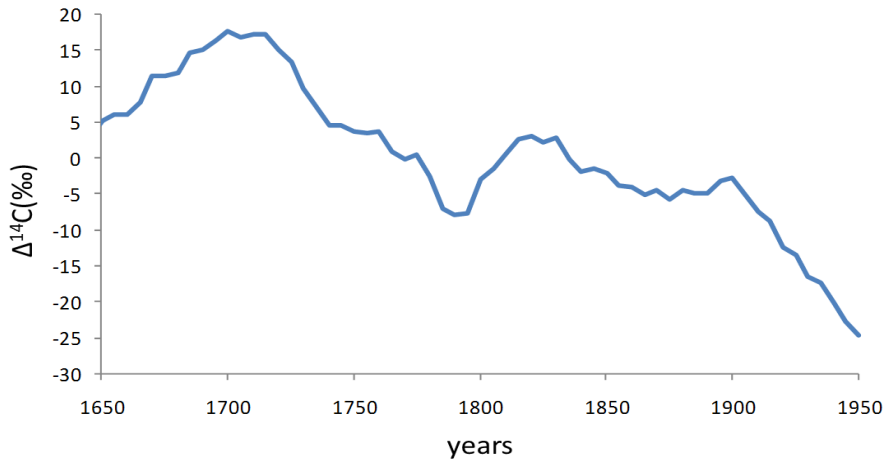

Figure 1.3 - Variation of radiocarbon concentration between 1650 and 1950; on the y axis, the variation is expressed as difference with respect to atmospheric concentration in 1950 [Rei2013].

Another anthropogenic effect, the so called “Bomb Peak”, has led to a significant change in the atmospheric radiocarbon concentration. After the Second World War, in particular during the late 1950s and the first 1960s, hundreds of nuclear weapon tests were performed in the atmosphere. During the explosions, a large amount of neutrons was produced, which after thermalising interacted with ^{14}N, almost doubling in a few years the radiocarbon concentration in the atmosphere. Then, in 1963 many countries stopped the nuclear arms race (signing the Test Ban Treaty) and few years later, in 1968, they finally signed the treaty on the Non-Proliferation of Nuclear Weapons [see e.g. Hua2009], putting an end to the nuclear explosions in atmosphere. Thus, in the following years, the radiocarbon concentration began to decrease again, in particular because of the exchanges among the different carbon reservoirs, mainly owing to a progressive “dilution” in the huge reservoir represented by the oceans. At the present days, the atmospheric radiocarbon concentration has almost recovered the pre-explosion levels, as shown in figure 1.4.

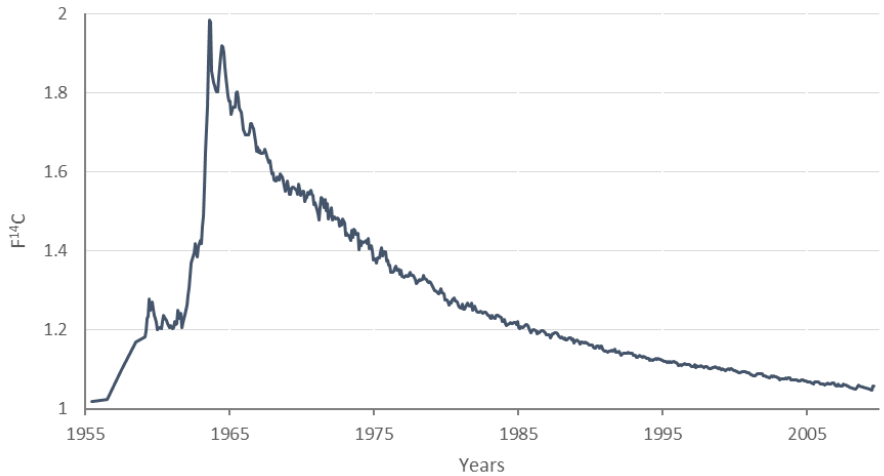

Figure 1.4 - “Bomb Peak” curve: on the y axis, the ^{14}C concentration is normalised to the concentration measured in atmosphere in 1950 [Hua2013].

Considering all these natural and anthropogenic variations, it is evident that $^{14}R_0$ in equation (1.4) is not really a constant. To solve the equation, and thus to obtain the conventional radiocarbon age, we necessarily have to choose a fixed value for $^{14}R_0$, but it is clear that, in this way, the radiocarbon age does not correspond to the real age

of a dated sample. This discrepancy can be overcome by indirectly "measuring" the variations of the ^{14}C concentration in atmosphere in the past, and using them to correct the radiocarbon ages, as described in paragraph 1.3.

1.2.3 Equivalence of ^{14}C concentration between the atmosphere and all the living organisms

In the conventional radiocarbon age, it is supposed that all the living organisms have the same radiocarbon concentration as the atmosphere, but also this hypothesis is true only to a first approximation. Indeed, biochemical processes are typically characterised by the so-called isotopic fractionation: they involve the preferential use of one isotope with respect to another; usually, the lightest isotope is favourite. For instance, during the photosynthesis process, the plants "prefer" ^{12}C to create C-C bonds: the abundance of ^{13}C and ^{14}C is thus lower in a vegetal organism than in atmosphere.

If we measure the radiocarbon concentration without considering the isotopic fractionation, the dated organism will therefore appear older. Since it is not possible to directly correct the effects of isotopic fractionation on ^{14}C because the concentration of this isotope changes according to its decay, the $^{13}C/^{12}C$ ratio is also measured in all samples: these two isotopes are stable and the variations of their relative abundances from sample to sample can be attributed only to fractionation. Thus, such an effect can be quantified and measured. The ^{13}C fractionation relative to ^{12}C in a sample is defined as:

$$\delta^{13}R = \left[\frac{\left(^{13}R/^{12}R\right)_{sample} - \left(^{13}R/^{12}R\right)_{VPDB}}{\left(^{13}R/^{12}R\right)_{VPDB}}\right] \times 1000 \qquad (1.5)$$

where $\left({}^{13}R/{}^{12}R\right)_{sample}$ and $\left({}^{13}R/{}^{12}R\right)_{VPDB}$ are the isotopic ratios of the sample and of the standard Vienna Peedee Belemnite (VPDB)[3], respectively [see e.g. Cop1994].

In Figure 1.5, the $\delta^{13}C$ of several materials are reported.

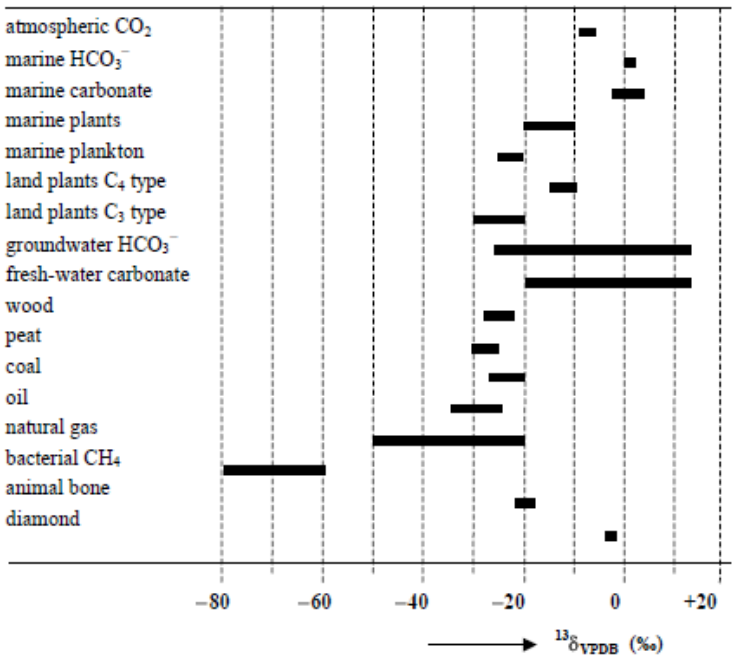

Figure 1.5 - Overview of the δ ^{13}C measured ranges due to isotopic fractionation in different natural materials (reproduced from [wIA2011]).

Assuming the relationship between ^{13}C and ^{14}C fractionation present in the literature[4] [Cra1954], it is possible then to correct the measured ^{14}C/^{12}C ratio as:

$$\left(\frac{{}^{14}R}{{}^{12}R}\right)_{sample,corr} = \left(\frac{{}^{14}R}{{}^{12}R}\right)_{sample,meas}\left(1 - 2\frac{25+\delta^{13}C_{sample}}{1000}\right) \qquad (1.6)$$

[3] VPDB is a fossil limestone from a crustaceous formation in South Carolina (USA).

[4] According to [Cra1954], we can evaluate the correction due to the ^{14}C isotopic fractionation as the square of the correction due to ^{13}C isotopic fractionation. Being these corrections sufficiently small, when developing to first order, we find the well-known rule: the ^{14}C fractionation is about the double of the ^{13}C fractionation, as shown in equation (1.6).

where $\delta^{13}R_{sample}$ is the isotopic fractionation of ^{13}C in the sample with respect to VPDB. The correction is evaluated normalising $\delta^{13}R_{sample}$ to the conventional value of -25‰, which corresponds to the mean isotopic fractionation of terrestrial wood and is approximately the value for all the plants that use the so-called C_3 process as the metabolic pathway for carbon fixation by photosynthesis.

1.2.4 ^{14}C in organisms living in marine and lacustrine environments

A variation of radiocarbon concentration also affects all the organisms that live in marine and lacustrine environments: in these cases, the organisms do not directly exchange CO_2 with the atmosphere, but with a different reservoir.

The oceans exchange carbon dioxide, that is water soluble, only on the surface, but, thanks to marine flows, $^{14}CO_2$ can be diffused into deep waters that are originally poor in ^{14}C. The diffusion process does not generate an equilibrium condition because the water masses are subjected to mixing phenomena. These are slow phenomena, whose characteristic times can be compared to radiocarbon mean life, thus they contribute to dilute the radiocarbon concentration present in the ocean. As a consequence, in case we neglect this effect, the marine samples show an apparent aging with respect to terrestrial organisms because their radiocarbon concentration is already lower, at the moment of death, than the one of the terrestrial organisms. As an average, this effect can be estimated as an aging of about 400 years.

The organisms living in lakes or rivers in basins that are particularly rich in calcium carbonate ($CaCO_3$) may experience a similar aging. Indeed, the dissolution of limestone, which is basically radiocarbon free, causes an increase of the ^{12}C atoms in the water and consequently a decrease of ^{14}C concentration. For an accurate dating of samples originating from these kind of environments, it is necessary to apply an appropriate correction taking into account this local effect.

1.3 The relevance of calibration of the radiocarbon age

In paragraphs 1.2.2 and 1.2.4, the variations of radiocarbon concentrations in atmosphere in the past and in some specific environments have been described. To take them into account, calibration curves have been built dating the same materials both by ^{14}C method and by some independent method, in order to relate the measured conventional radiocarbon age with the "true" calendar age.

In the 1960s, one of the first methods used to build the calibration curve was the comparison with dendrochronology. This dating method is based on the analysis of the patterns of tree rings widths. It is well known that many kinds of trees add a new growing ring every year: only the external one is in an equilibrium condition with the atmosphere as far as the carbon exchanges are concerned. Measuring the ^{14}C concentration in each ring, the atmospheric variations are thus "recorded" year by year. In this way, a calibration curve was progressively built, going back in time - nowadays - to about 12000 years ago. In order to extend the curve, other independent methods have been used. So, materials as corals, foraminifera and varves have been dated using e.g. Uranium/Thorium series. This has allowed us to obtain a calibration curve back to about 50000 years ago. The results of these independent methods are summarised in the so-called IntCal13[5], the calibration curve used by the international community in the case of terrestrial organisms.

As explained in paragraph 1.2.4, in the ocean waters, the radiocarbon concentration is lower than in the atmosphere. The international community has decided to construct a "general" marine calibration curve (Marine13) assuming constant reservoir corrections, used to calibrate the radiocarbon conventional age for samples of this kind of environments [Rei2013].

[5] Calibration curves are periodically updated improving the accuracy and the precision of the results. The most recent publication, accepted by the international community, is "IntCal13 and Marine13 radiocarbon age calibration curves 0-50,000 years cal BP" [Rei2013].

Figure 1.6 shows a portion of IntCal13. It is clear that its trend is not regular (it is actually full of wiggles); for this reason, the calibration of a conventional radiocarbon age may not correspond to a unique result.

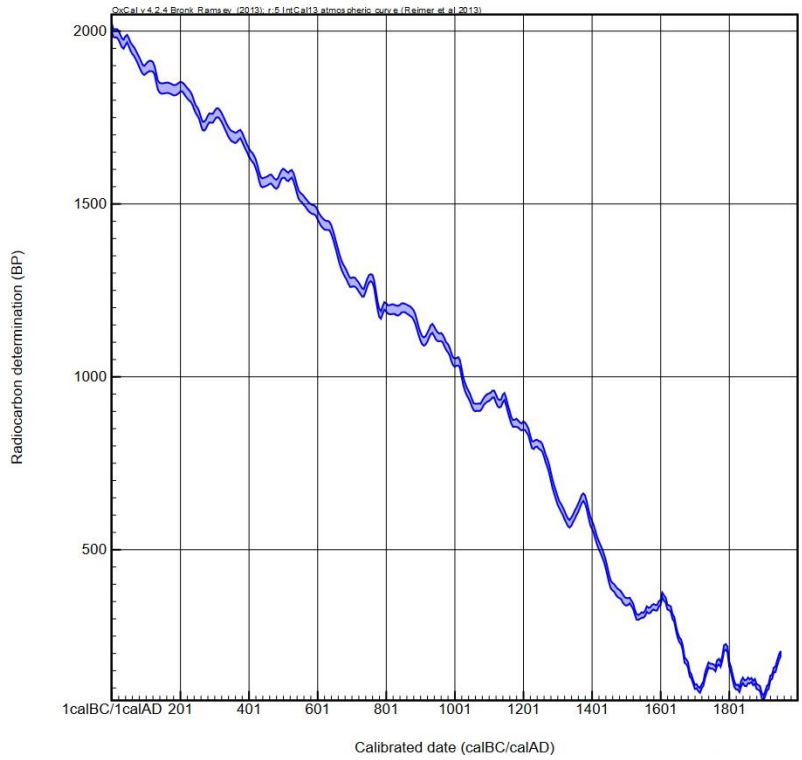

Figure 1.6 - The calibration curve IntCal13, reflecting the variations of radiocarbon concentration in atmosphere during the centuries: portion of the curve for the last 2000 years. The conventional radiocarbon age (t_{RC}) and the calibrated "real" date are represented on the y axis and on the x axis, respectively.

When we think about the result of a radiocarbon concentration measurement, we clearly think about a best estimate plus minus an experimental uncertainty: but not all the years in the radiocarbon age range are equally likely: they are distributed in a normal way, i.e. with a gaussian distribution. Correspondingly, not all the dates in the range of calendar years are equally likely. Owing to the non-linearity of the calibration curve (and to its intrinsic and variable uncertainty, as shown by the finite width of the calibration "line") the distribution of the calibrated dates obtained is no more gaussian. In order to correctly perform the calibration of a conventional

radiocarbon age, some software that takes into account all such effects has been developed. One of the most widespread programs is OxCal, developed by the Oxford Radiocarbon Accelerator Unit. In Figure 1.7, an example of calibration is shown using OxCal 4.2.

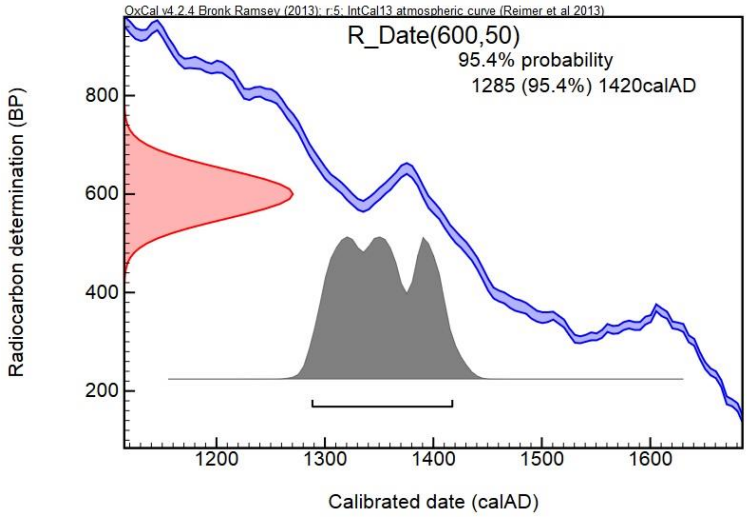

Figure 1.7 - Calibration of the radiocarbon age 600 ± 50 years BP (normally distributed, as shown by the pink curve on the y-axis): the calibrated date is in a range between 1290 and 1420 (at 95% confidence level) with the probability distribution shown by the full grey area.

The blue curve represents the calibration curve with its experimental error. The measured radiocarbon age is represented on the y axis as a Gaussian-distributed variable (in red in the figure), while the calibrated date (calendar age) is determined "projecting" the Gaussian distribution on the calibration curve. Typically, the result is represented as a distribution of probability (represented in grey). Once decided the confidence level (typically 68% or 95%), an interval of years is calculated corresponding to that level of confidence[6].

[6] Since the trend of calibration curve is irregular, it is also possible that more intervals of calendar ages correspond to the same measured radiocarbon age.

1.4 The hypothesis of the closed system and the issue of contamination

One of the main prerequisites for a reliable radiocarbon dating is that the sample to be dated have been a closed system since the death of the organism. Since carbon is a very common element, there is always the possibility of an exchange with the environment. Thus, it cannot be a priori excluded that the samples may have some contamination that must be removed before the measurement.

Contamination can be due either to "dead" carbon, poor in ^{14}C, or to "modern" carbon, rich in ^{14}C. As a consequence, in both cases, the measured radiocarbon age will not be the real one. Indeed, if "dead" or fossil carbon, where the radiocarbon concentration is basically zero, i.e. under the sensitivity limit of any measurement technique, contaminates a sample, its measured radiocarbon age appears older than the true one. In fact, the contaminant causes a sort of dilution effect. In the opposite case, if in the sample there is a fraction of modern carbon, i.e. with the same atmospheric radiocarbon concentration, its radiocarbon age will appear younger.

Exogenous carbon can affect findings for natural or anthropogenic causes. The typical sources of natural contaminations, especially for samples recovered in archaeological contexts, are represented by calcium carbonate, that can precipitate on the sample during the dissolution of limestone (dead carbon), and by humic acids[7] that are derived from the biodegradation of dead organic matter (basically modern carbon).

The term anthropogenic refers to contaminations caused by human operation, as, for example, the materials applied during a previous restoration. For instance, in the case of the restoration of paintings, the employment of organic compounds as egg, or several kinds of oil and waxes, in order to brighten up tones and colours, has been

[7] Humic acids, present in the soil, represent a complex mixture of many different acids containing carboxyl and phenolate groups.

very common since ancient times. Moreover, the use of various glues to strengthen the support or consolidate the material is a widespread procedure.

1.4.1 The particular case of contamination by fossil carbon

As stated in paragraph 1.4, if the contamination is due to "dead" carbon, the measured sample will appear older than expected. The relation between the measured radiocarbon concentration $^{14}R_{meas}$ and the fraction x of dead carbon can be expressed as:

$$^{14}R_{meas} = \frac{1}{1+x} \cdot {}^{14}R_0 e^{\left(-\frac{t_{true}}{\tau}\right)} \qquad (1.7)$$

where t_{true} is the true radiocarbon age.

The apparent radiocarbon age t_{app}, that we measure if the contamination is not removed, is thus:

$$t_{app} = \tau \, ln \frac{^{14}R_0}{^{14}R_{meas}} = t_{true} + \tau \ln(1+x) \qquad (1.8)$$

From equation 1.8, it can be seen e.g. that already for 1% of fossil carbon contaminant, an apparent aging of approximately 80 years is introduced. The contamination effect is not dependent on the true age of the sample, but this effect is more relatively more important for recent samples.

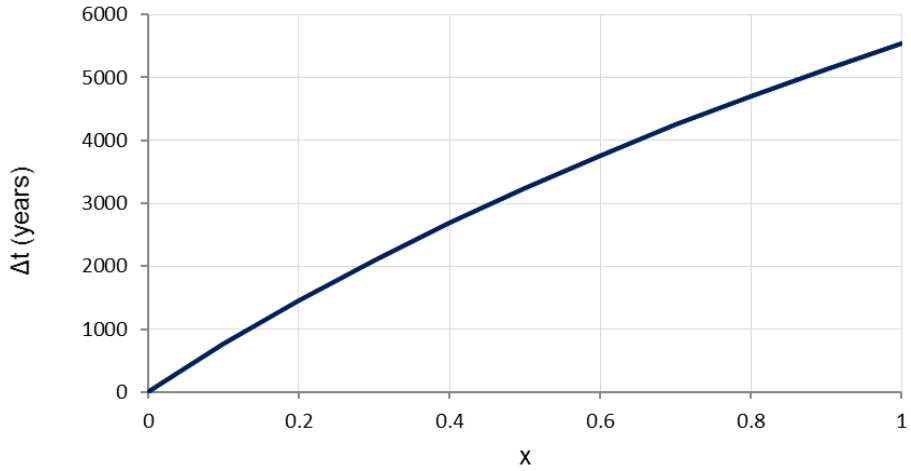

Figure 1.8 - Apparent aging as a function of the fraction x of contamination present in the sample. On the y axis the difference between the "apparent" radiocarbon age and the "true" one ($\Delta t = t_{app} - t_{true}$) is represented.

When, in the 1960s, industries selling chemicals for restoration introduced products that were based on synthetic resins, many operators began to apply them. These products, characterized by a better stability over time with respect to the natural ones, are usually produced by polymerization processes of fossil oil and/or its by-products [Hor2010]. Since hydrocarbons are devoid of ^{14}C, these kinds of products can represent a source of contamination by dead carbon, if they are not completely removed from the samples to be dated.

In particular, during my PhD work, I focused the attention on the problem of possible contamination due to Paraloid B72®, a very widespread synthetic resin used in the restoration field (see paragraph 3.2).

1.5 Identification of possible contaminants

The possibility to check the presence of contaminants in a sample to be radiocarbon dated would be very useful as a preliminary screening to choose the most specific procedure to remove them. When the samples to be dated have been restored, such precious information can be achieved talking with the restorers or looking in the

archives. However, these data cannot be always available. When any information cannot be recovered, an independent technique should be exploited to verify the possible presence of exogenous carbon.

The study and the characterisation of organic contaminants are possible first of all identifying the molecules that constitute the material. In order to investigate the compounds, several techniques can be used. Among the spectroscopic techniques, i.e. those techniques that study the interactions between electromagnetic radiation and matter, IR spectroscopy is the most accessible and well established [McD1978]. The electrons of the covalent bonds in a molecule react to quantised energies according to the vibration and rotation movements of molecules. These movements can be easily induced using radiation at the infrared wavelenghts. Most of the compounds respond to this range of electromagnetic radiation and characteristic spectra can be acquired. These spectra are specific of the bond complex of the molecules. One of the great advantages in the family of IR spectroscopic techniques is that they allow us to analyse quite simply samples in solid, liquid and gaseous states.

The most common method is the Fourier Transform Infrared Spectroscopy[8] (FT-IR). In the FT-IR technique, when the molecules are excited using infrared radiation, the vibrational and rotational motions are stimulated. If a change in moment dipole takes place in the molecule, an IR absorption can occur. In the spectrum, the absorption bands are attributable to specific movements of bonds, and this allows us to identify the specific bond in the molecules. Among the advantages of FT-IR technique, one can mention the rapidity of the analysis and the possibility to manage samples of small masses. In particular, the latter is surely a great advantage when dealing with samples collected in the Cultural Heritage field.

This method can require an elaborate sample preparation that depends on the nature of the sample itself. However, when the samples are in the solid state, it is sufficient to mix a few milligrams of sample with a support (typically Potassium Bromide - KBr) transparent to the IR radiation, to form a pellet. The analysis is a bulk

[8] See the appendix for a more detailed description of FT-IR technique

measurement on the sample, but hardly can the sample used to acquire the FT-IR spectrum be also used for another kind of analysis. In the case of detecting a contamination in a sample to be radiocarbon dated, the possibility to realize a bulk analysis is an advantage. In fact, a homogeneous distribution of contaminants is not usually found in the restored material.

The problems about sample preparation and the possibility to realize different analyses on the same sample can be overcome using Attenuated Total Reflectance (ATR) [Fri1999]. This technique is part of the infrared spectroscopy family as well, but it uses the mechanism of beam reflection on a high refractive index crystal placed into contact with the sample. ATR can only analyse the surface of the sample: the investigated thickness is about 2-3 μm. In the case of the identification of organic contaminants in a sample to be radiocarbon dated, as the possible contamination cannot be homogenous in the whole sample, a single ATR spectrum may not be representative of the whole sample itself.

In an analytical chemistry laboratory, another widespread technique that can be used to analyse the composition of possible contaminants is gas chromatography-mass spectroscopy (GC-MS). This technique is useful to separate and analyse the compounds in the field of Cultural Heritage, and it is often used to identify varnish, waxes, lipid and protein materials used as binders [Col2000]. Typically, the sample is solubilized in a suitable solvent or introduced into the instrument as gas. For the analysis, the gaseous compounds are moved by a mobile phase (gas carrier) through a column filled with a specific polymeric film that adsorbs and releases the different gases at different times depending on their affinity with the polymer itself. This process permits to the mass spectrometer allocated at the end of the column to analyse the ionised molecules separately. Surely, the combination of gas chromatography and mass spectrometry is very powerful for the identification of organic compounds [Col2009, Tam2014].

Among the mentioned techniques, during my PhD course, we have decided to investigate the possibility to use FT-IR as a support to the ^{14}C measurements. FT-IR is

here proposed as a diagnostic tool during the sample preparation phase, first to possibly identify the presence of contamination in the treated sample and then to control the removal process.

2. Radiocarbon measurements: experimental setup

The radiocarbon dating method always requires that a sample be collected from the find to be analysed, therefore it is a destructive process. Considering that radiocarbon dating is often applied to samples of archaeological and historical-artistic interest, collecting a small quantity of material is mandatory. Accelerator Mass Spectrometry (AMS) is a very sensitive technique that allows us to detect and count ^{14}C atoms with sufficient statistics even from tiny quantities of material. Prior to AMS measurement, however, sample preparation, and in particular the pre-treatment, is a fundamental step to remove possible contaminations.

2.1 Accelerator Mass Spectrometry (AMS)

To determine the conventional radiocarbon age (see equation 1.4), the most straightforward way is directly counting the residual number of ^{14}C atoms. In principle, we may think to apply a typical mass spectrometric approach. However, traditional mass spectrometry is not useful, because it cannot discriminate radiocarbon from the isobaric interferences that are more abundant than ^{14}C itself. Beyond the

interference of ^{14}N, the most common element in atmosphere[1], there are two important interferences due to molecules characterised by the combination of H and ^{12}C or ^{13}C (namely ^{13}CH and $^{12}CH_2$). The sensitivity of a traditional mass spectrometer can be at the very best of one part in 10^{10}, while the abundance of ^{14}C is only about $1.2 \cdot 10^{-12}$ in a modern sample (and obviously lesser and lesser in increasingly old samples). The use of Accelerator Mass Spectrometry (AMS) allows us to increase the sensitivity even to one part in 10^{15}, making the detection of ^{14}C atoms possible. The key is exploiting several magnetic and electrostatic filters combined with a Tandem electrostatic particle accelerator, to separately count ions of mass 12, 13 and 14. The name Tandem of the accelerator depends on the fact that the charged particles are accelerated in two subsequent phases.

Samples to be dated are inserted in the accelerator source[2]: a negative ion beam is extracted. In this way, the main interference due to ^{14}N is removed: indeed, the stable isotope ^{14}N can form negative ions but in excited states, whose mean lifetimes are too short to survive until be injected into the accelerator. Thus, the source itself acts as a filter, suppressing the N interference. After the source, the beam is analysed according to the different masses through a series of electrostatic and magnetic fields and then accelerated. As it will be described in the next paragraphs more in details, the molecular isobars are suppressed during the so-called stripping process at the high voltage terminal. After the acceleration, additional analyses are performed using a magnet and an electrostatic analyser. Measuring the abundances of the three carbon isotopes, $^{14}C/^{12}C$ and $^{13}C/^{12}C$ ratios can be determined.

The ^{14}C-AMS measurements for this work were performed at the Tandem accelerator installed at INFN-LABEC (Laboratorio di Tecniche Nucleari per l'Ambiente e i Beni Culturali) laboratory in Florence.

[1] Actually, Nitrogen represents about 78% of gas present in atmosphere.

[2] Of course, before being inserted into the source, samples undergo a careful preparation process to remove all the possible contaminations and to convert their carbon content in the most appropriate chemical form (see paragraph 2.2.1).

2.2. Sample preparation for radiocarbon dating

As mentioned in paragraph 1.4, before the measurement of radiocarbon concentration, samples must be subjected to a pre-treatment procedure in order to eliminate all exogenous carbon that might be present in the material. If this does not happen, we will obtain measurements affected by systematic errors. During the pre-treatment process, the samples lose a part of their mass: the amount of such a loss depends on the nature of the sample itself and on its state of preservation. Typical masses of the processed samples are of the order of few tens of mg[3], much larger than the masses of the measured graphite pellets that are inserted into the accelerator ion source (order of some hundreds of μg). The successive steps in the sample preparation procedure are the combustion and the so-called graphitisation, which convert the carbon in the sample to graphite powder (to finally obtain the graphite pellets to be inserted in the source, paragraph 2.3.1)

2.2.1 The pre-treatment process

The first step of the sample pre-treatment is a mechanical cleaning through tweezers and scalpel in order to remove the outer layers of the material. These surfaces have been in contact with the external environment and so they are the most vulnerable to possible exchanges with contaminants. For example, in the case of samples collected in an archaeological excavation, the outer layers are in direct contact with the soil, which can be rich in carbonates and humic acids, as reported in paragraph 1.4. In some cases, samples can present macroscopic crusts that cannot be eliminated simply by the scalpel, but may be removed by ultrasonic bath in deionized water. After this "mechanical" cleaning, to maximize the available surface for the subsequent chemical attack, the samples are divided into fragments as small as

[3] Masses of about 20 mg at most are typical in the case of, for example, wood and textiles; in some other cases, when the sample matrix is complex, a larger mass may be required, as in the case of bones (usually, about 500-1000 mg).

possible: for example, in the case of wood, they are cut into very small chips, while bones are ground to obtain a fine powder.

Subsequently, the samples are typically treated using chemical solutions depending on the fraction that has to be extracted and dated. Since the kinds of material to be dated are so diverse, it is not possible to apply a unique pre-treatment procedure. Furthermore, the state of conservation of the processed material must be considered case by case. For example, if the material is particularly deteriorated, the chemical approach will be more gentle.

When the possible contaminations are natural, the pre-treatment is focused to essentially remove carbonates and organic soil traces, and the so-called ABA treatment (Acid -Base- Acid) is used [Sou2010]. ABA treatment is developed according to the following steps:

- Bath in aqueous HCl solution;
- Bath in aqueous NaOH solution;
- Bath in aqueous HCl solution;
- Heating in oven until complete dryness.

The first bath in acidic solution allows us to dissolve carbonate residues according to the reaction:

$$CaCO_3 + 2HCl \rightarrow CaCl_2 + H_2O + CO_2 \qquad (2.1)$$

Usually, the acidic solution concentration is chosen as 1M. If the material is in a good preservation state, the bath takes place at about 80°C.

This first step in HCl is fundamental especially in the case of bone samples, when our aim is at extracting collagen, the suitable fraction to be dated. Several baths in HCl, lasting up to 24 hours, are required completely demineralise the bone matrix.

The second step, the bath in alkaline solution, favours the removal of humic acids that can be present. For some materials, especially those that are composed of some proteins as keratin, e.g. silk and wool, this stage is a tricky phase. Indeed, it is well

known that the degradation of the proteins can be favoured by an alkaline environment. For other materials, in general, a 0.1M solution is used. During this phase, atmospheric CO_2 can dissolve in the bath, so an additional bath in HCl is typically performed as a further step. At the end of each step, the sample is washed using deionized water in order to obtain neutral pH.

The simple mechanical cleaning of the sample and the ABA pre-treatment are not effective to remove all kinds of contaminations, especially in the case of synthetic products used in restoration. In these particular cases, it is necessary to find a more specific method that can totally eliminate the exogenous carbon without becoming however a source of contamination itself, releasing carbonaceous residues (see paragraph 3.3).

2.2.2 The combustion of the sample

Once the pre-treatment is concluded and the sample can be assumed to be clean, it is necessary to extract only the carbon fraction. At LABEC, an elemental analyser (EA, Thermo Flash 1112) is used to burn the sample and to separate CO_2 with respect to the other gases derived from the combustion [Min2010].

The instrument is setup to measure Carbon, Hydrogen and Nitrogen abundances (CHN configuration). The EA is equipped with an autosampler. The autosampler is a carrousel where up to 32 tin capsules, containing the material to be burnt, can be allocated. The capsule containing the sample to be burnt is dragged by a shaft to a position from which it falls down into the combustion column. This shaft is equipped with some O-rings to allows the volume inside the autosampler and the combustion column to be saturated with Helium, which is the gas carrier through the whole path inside the EA. The EA furnace, kept at a temperature of about 900°C, is composed by a quartz column, where a flash combustion, triggered by the injection of Oxygen, takes place at a temperature of about 1100°C. The quartz column is filled with different solid reagents (chromium oxide, copper, silvered cobaltus oxide) which contribute to oxidise and reduce the gases produced by the combustion. Nitrogen

oxides are reduced by Cu, while any sulphur trace is absorbed by silvered cobaltus oxide. This sulphur trap is fundamental because the sulphuric compounds can otherwise inhibit the successive graphitization reaction.

Out of the furnace, the three gaseous components (N_2+CO_2+H_2O) pass through a gaschromatographic column. At the end of this column, there is a thermal conductivity detector (TCD) that measures the output gases. At the detector terminals, a voltage is measured depending on the kind of gases flowing from the gaschromatographic column. Thus, the signal is acquired by a PC-board and displayed in a so-called chromatogram (see Figure 2.1). The detector signal is plotted as a function of time: the different gases reach the end of the column at different times, producing a peak in the spectrum; the area of each peak is proportional to the amount of the corresponding gas.

In our setup, the outlet of the elemental analyser is coupled to a 3-way valve. One of the exit ports of the valve is open to air and for most of the time the gases exhaust through this port; only for the time interval during which CO_2 is transmitted at the output of the gaschromatographic column, the valve is instead switched to a port that is connected to the graphitization line downstream, so that the CO_2 is let to flow into that line, to be trapped for the following preparation step.

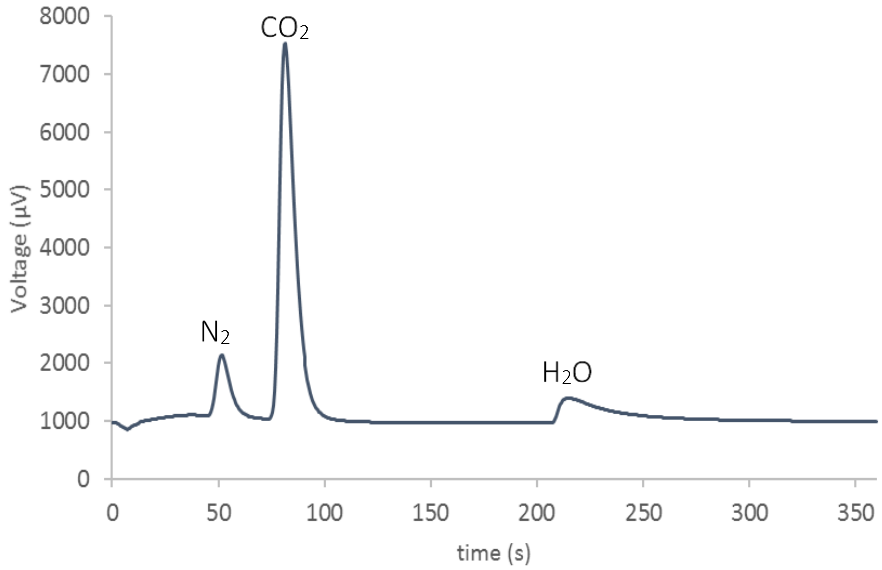

Figure 2.1 - Example of chromatogram of cyclohexanone-2,4-DNPH ($C_{12}H_{14}N_4O_4$). N_2, CO_2 and H_2O gases flow out of the gaschromatographic column at different times.

2.2.3 The graphitization process

In Figure 2.2, the outline of the combustion and graphitisation line is shown. As already mentioned, the elemental analyser is joined to the graphitisation line via a 3-way valve. When carbon dioxide is starting to exit the gaschromatographic column, as can be checked in the chromatogram, the operator switches this valve: CO_2 and He flow through a capillary into the graphitisation line.

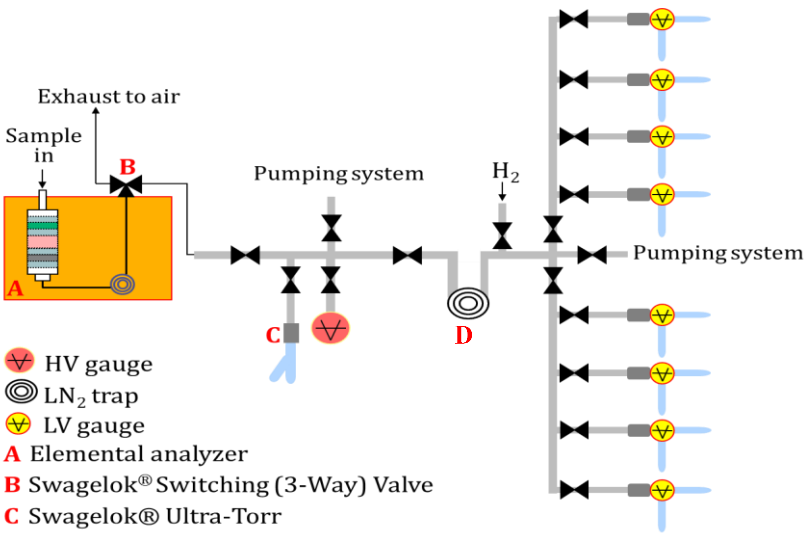

Figure 2.2 - Schematic layout of the combustion and the graphitisation line. The 3-way valve (B) allows the transfer of the CO_2 and the gas carrier (Helium) into the line. The coil (D) is kept in liquid nitrogen to cryogenically trap CO_2, while the pumping system is open in order to remove He. Then, CO_2 is heated and transferred in one of the reaction chambers. Here, Hydrogen is added to allow the graphitisation reaction occurring.

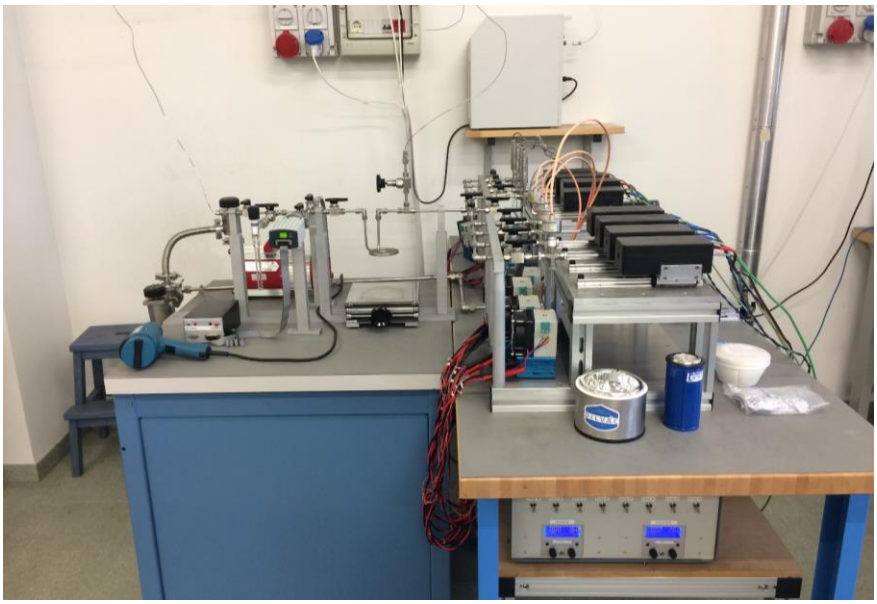

Figure 2.3 - Graphitization line installed at LABEC.

Before any operation, the line is evacuated, at a pressure of about 10^{-4} mbar. With reference to Figure 2.2, while the mixture CO_2 and Helium is flowing from the elemental analyser, the coil D is plunged in a LN_2 trap, in order to freeze the CO_2. When all the CO_2 derived from the combustion has flown, the 3-way valve is switched again to open air, preventing the transmission of the other gases to the line downstream. Since Helium does not condense at the liquid nitrogen temperature (about -196°C) it can be then pumped out by reopening the valve of the pumping system. Afterwards, when Helium is completely removed (as can be monitored through the pressure gauge), the operator isolate again the line from the pumping system and the coil is extracted from the N2 bath and heated, in order to let the CO_2 expand in the line. Eight reaction chambers are currently installed. Each reaction chamber is composed of two quartz tubes and is isolated from the line through a valve. CO_2 is converted into graphite, the elemental carbon, according to the reaction [Vog1984]:

$$CO_2 + 2H_2 \xrightarrow{\text{Fe,600°C}} C + 2H_2O \qquad (2.2)$$

The reaction takes place with iron powder that acts as catalyst. The tube containing the catalyst is inserted in an oven at the temperature of about 600°C. At the same time, the second tube is inserted in a cooling device[4], kept at the temperature of about -25°C. Indeed, the secondary product of the reaction is water that, if not removed from the gas phase, would progressively feed the inverse reaction. In this way, instead, the water produced is maintained in the solid phase and the reaction can proceed until the complete reduction of all the CO_2 molecules to form graphite.

During the graphitisation process, the reaction trend is monitored using a pressure gauge installed in the chamber. After about two hours and half, when the chamber

[4] The cooling system is based on the Peltier effect: a thermoelectric junction can transfer heat from one side to the other depending on the direction of the current.

pressure has reached a minimum and constant value[5], the reaction is complete and a graphite (+ iron) powder is obtained.

The catalyst is inserted in an oven at the temperature of about 600°C. At the same time, the second tube is inserted in a cooling device[6], kept at the temperature of about -25°C. Indeed, the secondary product of the reaction is water that, if it is not removed, can trigger the reverse reaction. In this way, the water is maintained in the solid form and the reaction can proceed forming graphite.

During the graphitisation process, the reaction trend is controlled using a pressure gauge installed in the chamber. After about two hours and half, when the chamber pressure has reached a minimum and constant value, the reaction is complete and the powder graphite sample is obtained.

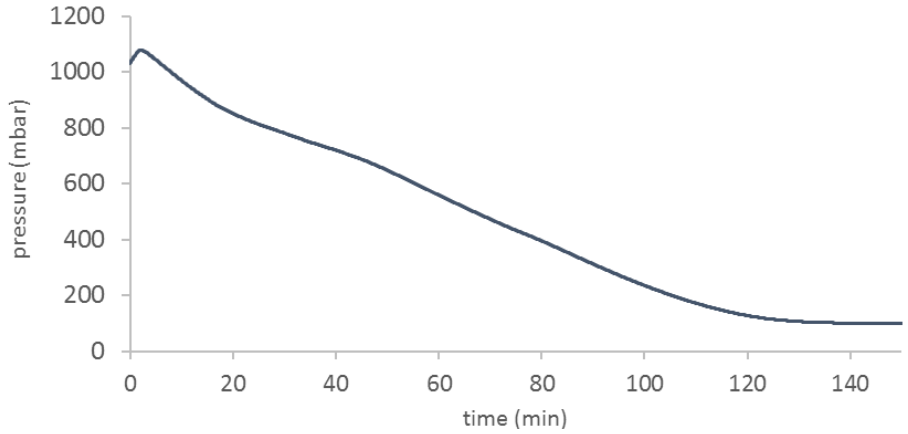

Figure 2.4 - Trend of the pressure in the reaction chamber during the graphitization process.

Finally, the mixture of graphite and iron powder is pressed is an aluminium support to be inserted in the AMS source (see paragraph 2.3.1) for radiocarbon measurement.

[5] The non-zero value of the final pressure steady-state is due to residual H_2: indeed, a slight excess of H_2 with respect to the stoichiometric quantity (i.e. twice the pressure of CO_2) is precautionally introduced at the beginning into the reaction chamber, to be sure of a total reduction

[6] The cooling system is based on the Peltier effect: a thermoelectric junction can transfer heat from one side to the other depending on the direction of the current.

2.3 The ^{14}C-AMS setup at INFN-LABEC

At INFN-LABEC, an electrostatic Tandem accelerator with 3MV maximum terminal voltage, operating since 2004, is installed [Fed2007]. The accelerator is equipped with three ion sources and 6 beam lines dedicated to Ion Beam Analysis (IBA) and AMS measurements.

The AMS beam line can be divided in three sections:

- Low-energy side: composed by the negative ion source and by the system of pre-analysis and ion injection into the accelerator;
- Tandem Accelerator: where the two-step acceleration mechanism takes place; after the first acceleration to the positive-high voltage terminal, the mechanism of stripping occurs within the terminal and the ions, now become positive, are further accelerated to the exit of the Tandem at ground potential;
- High-energy side: where the measurement of ^{12}C and ^{13}C abundances and the further analysis and detection of the rare isotope ^{14}C occur.

A schematic layout of the Tandem accelerator at INFN-LABEC is shown in Figure 2.5

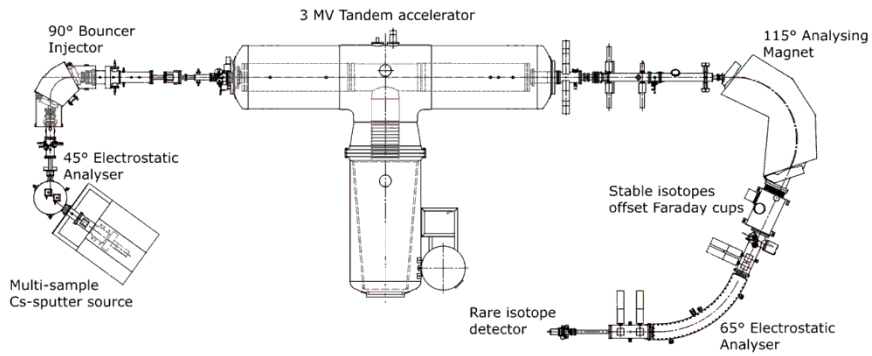

Figure 2.5 - Schematic layout of the AMS beam line at INFN-LABEC (the ion sources and the different beam lines dedicated to IBA measurements are not shown in the figure).

2.3.1 The low energy side

The sample to be measured, pressed into a circular hole of an aluminium support (called colloquially cathode) and in the solid form of graphite (mixed with the iron catalyst powder), is introduced in the Cs-sputter negative ion source. The source is equipped with a wheel that allows positioning up to 58 samples. Using an air-actuated mechanism, each sample can be allocated into the sputtering position, which is on a x-y movable stage. During the measurement, this stage can micrometrically move the target in different positions, in order to sputter the whole surface and prevent the possible formation of craters in the graphite pellet.

Inside the source, a reservoir filled with caesium, alkaline metal with a very low melting point (28.4°C), is heated up to about 80°C: in this way, Cs forms vapours that come into contact with a hemispherical surface, the so-called ioniser, heated to high temperature (about 1100°C). When hitting the hot surface, Cs forms positive ions owing to the mechanism of thermal ionization. These ions are accelerated towards the cathode sample surface, which is kept at a voltage of -7kV with respect to the ionizer. The Cs ions bombard the cathode surface causing the extraction of molecular fragments and atoms (sputtering process). In addition, a thin layer of Cs ions settles on the sample surface that is kept at a lower temperature: when the sputtered particles cross this layer, they acquire electrons becoming negative ions. The by far most probable charge state is q=-1.

The negative ion beam is then extracted from the source thanks to an applied voltage of few tens of kV, specifically 35 kV in the case of LABEC facility.

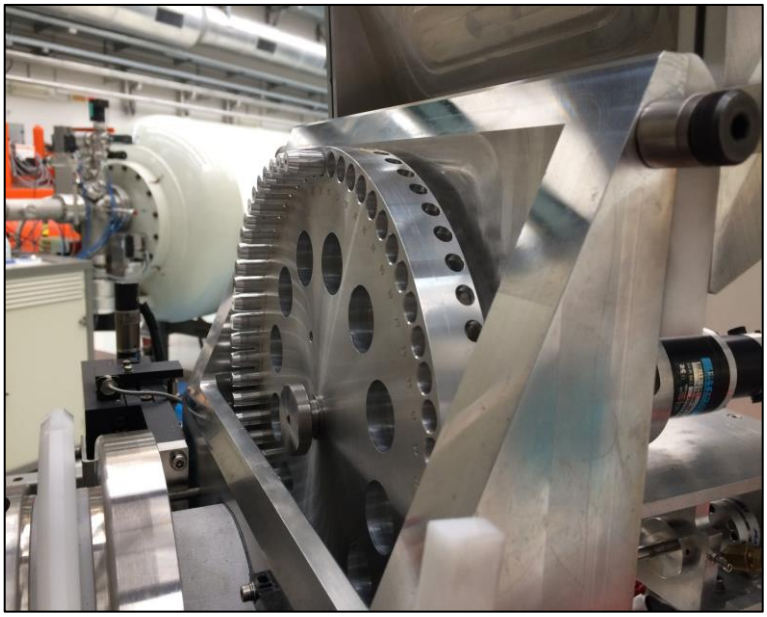

Figure 2.6 - Details of the wheel with graphite samples pressed in the aluminium supports for the measurement.

At the exit of the source, the beam crosses the first analyser element (electrostatic analyser, ESA) in order to select those fragments which have the appropriate energy/charge ratio. The electrostatic analyser consists in two concentric cylindrical electrodes, between which a large potential difference is applied. Because the bending radius *r* of the ESA is fixed by the construction geometry, the particles can be selected changing the applied voltage, and then the electric field to the plates, according to:

$$\frac{E}{q} = \frac{r \cdot \varepsilon}{2} \tag{2.3}$$

where E and q are respectively energy and charge of the ions, ε is the modulus of the electric field. In the case of a ^{14}C measurement, we select particles with the fixed ratio of energy/charge (E/q) considering charge of -1 and energy of 35keV, corresponding to the energy acquired during the extraction from the source.

The purpose of the second element of analysis, a fixed 90° magnet, is to select the ions with desired mass having fixed energy and charge. According to the following equation, the desired masses 12, 13 and 14 are selected:

$$Br = \frac{\sqrt{2mE}}{q} \qquad (2.4)$$

where r is the magnet bending radius, B is the magnetic field, m, E and q are respectively mass, energy and charge of the ions.

During the measurement, the three different masses 12, 13 and 14 are transmitted in cyclical mode, one after the other. The magnetic field B is kept constant so as to avoid hysteresis effects that can happen during the repetition of successive cycles. Since the trajectory r is fixed by the construction geometry, in order to transmit different masses, the energy of particles is changed. This is possible applying a proper voltage to the magnet vacuum chamber, that is in fact electrically insulated with respect to the beam line. Changes in the applied voltage can be arranged in a way that is faster with respect to changes in the magnetic field. In this facility, the magnetic field is set to transmit mass 13, while to transmit the other masses the proper voltage is applied. Each mass passes through the magnet for an appropriate period: obviously ^{14}C is favoured because its abundance is several order of magnitude smaller than the abundance of the two stable isotopes. So it is transmitted for most of the time. The cycle is composed by these duration intervals:

- Δt_{14}=8.5 ms;
- Δt_{13}=0.6 ms;
- Δt_{12}=6 µs.

Considering a transition time of about 250 µs between any state of voltage and the successive, the complete cycle of injection is about 10 ms.

At the exit of the magnet, the molecular interferences are still present: the beam is then injected into the accelerator, which also acts as a further filter.

2.3.2 The accelerator

In the electrostatic accelerator installed at LABEC, the high voltage at the terminal is produced by a cascade generator, whose operation is similar to a Cockroft-Walton voltage multiplier, based on a stack of capacitors and diodes. In this facility, the maximum achievable voltage is 3 MV. To stand such high voltages, the high voltage generator, the terminal and the accelerator tube are located in a tank filled with an insulating gas (Sulphur Hexafluoride -SF_6- at a pressure of about 6 bar).

Negative ions transmitted by the injector magnet are accelerated towards the terminal that is typically kept at 2.5 MV (V_t), during AMS measurements. The ions energy is increased: $E=E_{inj} + e \cdot V_t$, where E_{inj} is the energy of the ions at the entrance of the accelerator (35 keV) and e is the elementary electronic charge. In correspondence to the terminal, the ions pass through a portion of channel (13mm diameter, 100 cm length) where argon continuously flows: the interaction between the thin "layer" of argon and the negative ions leads to the removal of electrons (stripping process). The ions are thus converted from negative to positive. The stripping process is dynamic and the ions can acquire any of the possible charge states with a certain probability (see Figure 2.7). The most probable one depends on several parameters, including the terminal voltage: at 2.5 MV, the most probable charge state for carbon is 3+.

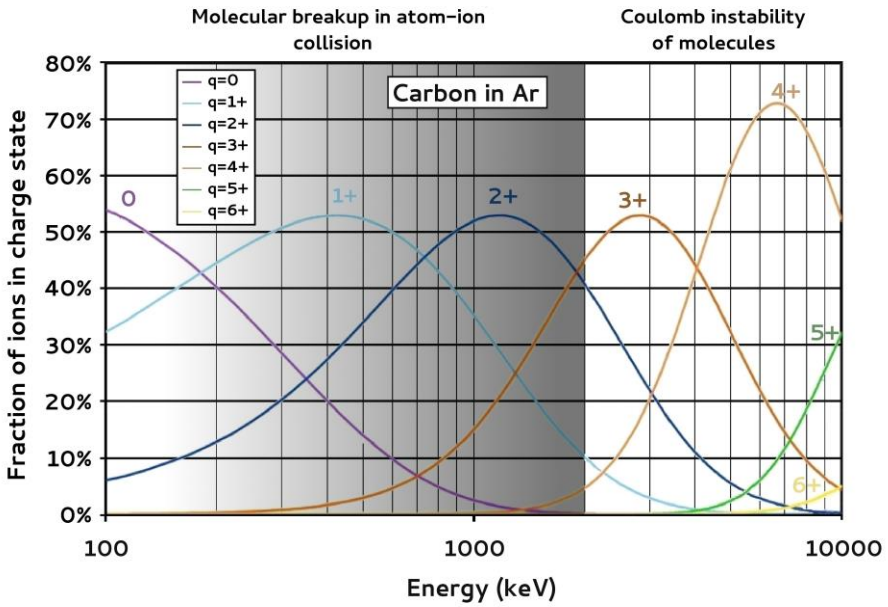

Figure 2.7 - Distributions of the possible charge states for carbon ions interacting in Ar depending on ions energy at the terminal. At 2.5 MV, which is the typical terminal voltage for ^{14}C-AMS measurements at LABEC, the most probable charge state is 3+.

After the stripping process, the positive beam is further accelerated to ground potential. Finally, at the exit of the accelerator, the energy of the ions is given by:

$$E_{fin} = \left(E_{inj} + e \cdot V_t\right) \cdot \frac{m_i}{m_{tot}} + qeV_t \qquad (2.5)$$

where E_{inj} is the energy of the negative particles before the injection, e is the elementary electronic charge, V_t is the terminal voltage, m_i is the mass of positive ions with charge state q and m_{tot} is the mass of the negative injected ion. The energy E_{fin} of the carbon ions, considering the most probable charge state 3+, is 10.035 MeV.

During the stripping process, another effect occurs: the interferences due to the isobars ^{13}CH and ^{12}CH$_2$ are suppressed. Indeed, passing through argon, these molecules lost the electrons breaking the molecular bonds, and they are eventually separated into their atomic components.

2.3.3 The high energy side

After the acceleration, for the further analysis, the beam passes through another magnet. This selective element is set to transmit only ions of mass 14, charge state 3+ and energy of about 10 MeV, according to (2.4).

During the injection time windows that allow transmitting the masses 12 and 13, the respective ions $^{12}C^{3+}$ and $^{13}C^{3+}$ are collected and measured in two specific Faraday cups that are installed on inner trajectories compared to $^{14}C^{3+}$ path, just after the magnet. Being acquired not in continuous way, but only when the masses are transmitted, the measured currents for the two stable isotopes are typically of the order of 1-10 nA.

After the magnet, the beam is basically composed by only $^{14}C^{3+}$.However, some particles with particular combinations of mass, charge state and energy may be transmitted through the magnet. For instance, this may be due to a stripping event, which occurred not exactly at the terminal. In order to remove such interferences, another electrostatic analyser is installed along the line. This ESA allows particles having the energy/charge ratio E/q=10.035MeV/3*e* to pass through. In this way, the magnet and the ESA acts as double filter.

With the aim at improving the sensitivity of AMS measurements on samples with ^{14}C ultra-low concentration, in the final part of beam line, a time of flight (TOF) system is installed. A TOF system can distinguish between particles with different masses, but having the same energy, measuring the times taken to cover a fixed path.

The possibility to perform TOF measurements at LABEC facility can improve the accelerator background and, at the same time, it can contribute to identify the presence of possible residual interfering particles [Pal2015].

2.3.4 Detecting ^{14}C

The typical ^{14}C counting rate that we can expect in the case of a modern sample ($^{14}C/^{12}C \sim 10^{-12}$) is only about 15 counts/s^{-1}, so a Faraday cup cannot be used to detect

the ^{14}C current as in the case of ^{12}C and ^{13}C. Even though it is well known that the exposure of a solid state detector, as a silicon photodiode, to charged particles can cause a significant deterioration of its performance, such a low counting rate permits the use of this device. A silicon photodiode detector is installed at the end of the AMS beam line at LABEC. The collected signal is amplified and acquired by a PC board in a spectrum only during the time interval Δt_{14} when mass 14 is injected into the accelerator. Figure 2.8 shows a typical spectrum collected during the measurement of a modern sample, i.e. rich in ^{14}C. The possible interferences are suppressed and only one peak is observed in the spectrum.

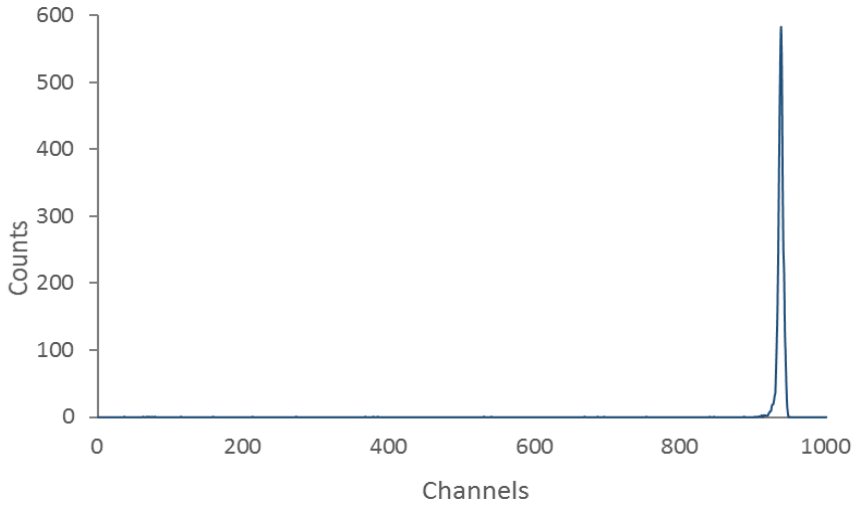

Figure 2.8 - Spectrum acquired for a modern sample, rich in ^{14}C, during a beam run (~ 270 s). The possible interferences are suppressed so that in the spectrum a single peak is well visible.

2.4 How to analyse the AMS data

During an AMS beam run, unknown samples (i.e. samples to be dated), together with primary and secondary standard and blank samples, are inserted in the same wheel in the accelerator source. Primary standard samples, which are characterized by a certified radiocarbon concentration, are measured to normalize the $^{14}C/^{12}C$ isotopic ratio of the unknown samples. As reference material, NIST Oxalic Acid II (SRM

4990C - National Institute of Standard and Technology, U.S.A.) with a certified radiocarbon concentration of 134.06±0.04 pMC [Man1983] is used. pMC (per cent of Modern Carbon) is one of the typical units to express the measured radiocarbon:

$$pMC(\%) = \frac{^{14}R_{sample}}{^{14}R_{ref}} \cdot 100 \qquad (2.6)$$

where $^{14}R_{ref}$ is the 95% of the radiocarbon concentration measured in Oxalic Acid I NBS (National Bureau of Standards) in 1950. This reference material is no longer commercially available and it is replaced with other reference materials, including the already mentioned NIST Oxalic Acid II [Ste2011].

The secondary standard IAEA C7 (International Atomic Energy Agency), whose certified radiocarbon concentration is 49.53 ± 0.12 pMC [Le1998], is used as a check of the accuracy in the measurements. Blank samples, whose radiocarbon concentration is nominally zero[7], are also measured, to correct for the background counts. Actually, being prepared and measured using the same procedure of the unknown samples, they allow us to verify whether some contaminations are introduced in the different preparation steps or in the accelerator itself.

To improve the measurement precision, when possible, two graphite pellets from each of the unknown samples are prepared. Once verified that the measured results are consistent, the best estimate of the radiocarbon concentration of each sample is determined as the weighted average of the two pellets values.

As mentioned in paragraphs 2.2.3 and 2.2.4, for each measured sample, ^{14}C counts and ^{12}C and ^{13}C currents are acquired. As already explained in paragraph 1.2.3, the measured $^{14}C/^{12}C$ isotopic ratios need to be corrected for the isotopic fractionation effect, so $^{13}C/^{12}C$ ratios are also acquired through the accelerator beam line. The contribution due to the background counts is subtracted from the $^{14}C/^{12}C$ isotopic

[7] At INFN-LABEC, as blank material, we use a chemical compound derived from fossil carbon: Santis Analytical Cyclohexanone 2,4-DNPH.

ratios measured for the unknown and standard samples. The normalised measured radiocarbon concentration, after the background counts and the isotopic fractionation corrections, is thus expressed as:

$$^{14}R_{\mathrm{t,pMC}} = {}^{14}R_{\mathrm{std,pMC}} \cdot \left(\frac{{}^{14}R_{\mathrm{t}} - {}^{14}\mathrm{R_{blk}}}{{}^{14}\mathrm{R_{std}} - {}^{14}\mathrm{R_{blk}}}\right) \cdot \left(\frac{{}^{13}R_{\mathrm{std}}}{{}^{13}R_{\mathrm{t}}}\right)^2 \qquad (2.7)$$

where $^{14}R_t$ and $^{13}R_t$ are the measured $^{14}C/^{12}C$ and $^{13}C/^{12}C$ isotopic ratios in the unknown samples, $^{14}R_{std}$ and $^{13}R_{std}$ are the measured $^{14}C/^{12}C$ and $^{13}C/^{12}C$ isotopic ratios in the standard samples, $^{14}R_{std,pMC}$ is the certified radiocarbon concentration of the standard and $^{14}R_{blk}$ is the measured $^{14}C/^{12}C$ isotopic ratio in blank samples.

Obviously, the radiocarbon concentration in the reference material also decreases according to the decay law, so, in order to obtain the radiocarbon concentration expressed in pMC as a time-independent measurement, $^{14}R_{sample}$ and $^{14}R_{ref}$ have to be measured at the same time.

3. Challenges in ^{14}C-AMS samples preparation

If the sample to be dated is suspected to be contaminated by materials used for restoration purposes, as the widely used Paraloid B72®, the pre-treatment process should be aimed at its complete removal. In this chapter, the new chloroform-based method to remove those contaminations is presented. In addition, possible cross-contaminations due to the sample preparation experimental setup are discussed.

3.1 Can the elemental analyser be a source of contamination?

An Elemental Analyser to collect the CO_2 from the samples to be radiocarbon dated is used not only at LABEC but it is also widespread in many other international laboratory setups [Sch2007, Wac2010, Lin2013]

Indeed, the EA has some unquestionable advantages. The main positive points are:

- the combustion of samples is fast;

- in the same time of burning, it is possible to measure the elements abundances that allow us to obtain quality indicators, as e.g. C/N ratios in the case of bone samples.

However, it is known that some parts inside the instrument may introduce cross contaminations and this can of course represent a drawback.

3.1.1 A cross contamination event

During a measurement beam run in the first year of my PhD course, radiocarbon concentrations higher than expected in blank samples were observed. Moreover, there was a large scattering in samples prepared from the same materials.

Figures 3.1, 3.2, 3.3 and 3.4 show the $^{14}C/^{12}C$ isotopic ratios measured for blank, primary standard (NIST Oxalic Acid II), secondary standard (IAEA C7) and two couples of unknown samples.

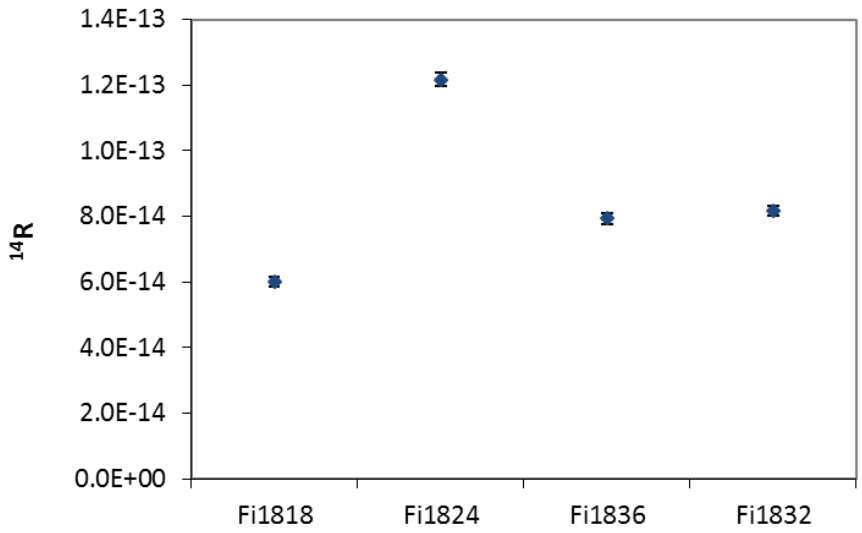

Figure 3.1 - $^{14}C/^{12}C$ isotopic ratios measured in blank samples are so high that they correspond to radiocarbon ages of about only 19000 years BP. Error bars are quoted at 1 sigma uncertainty for all samples.

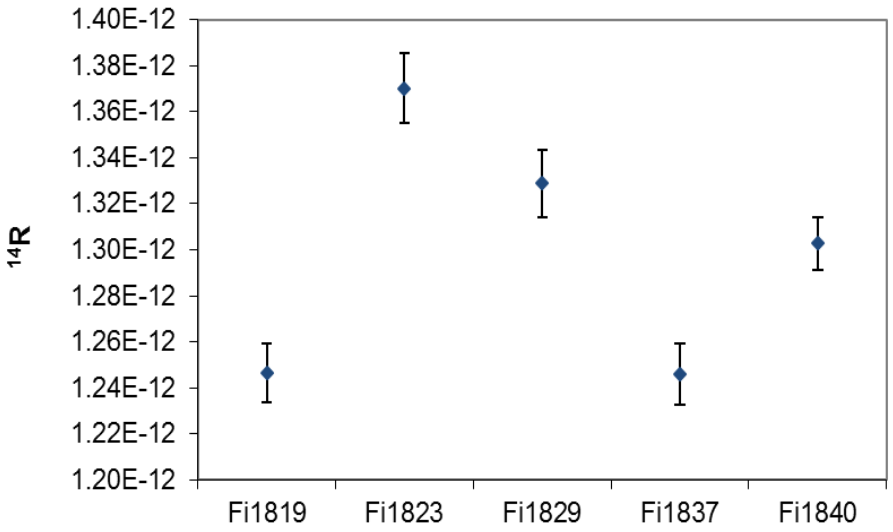

Figure 3.2 - $^{14}C/^{12}C$ isotopic ratios measured in primary standard samples (NIST Oxalic Acid II) showing largely scattered values.

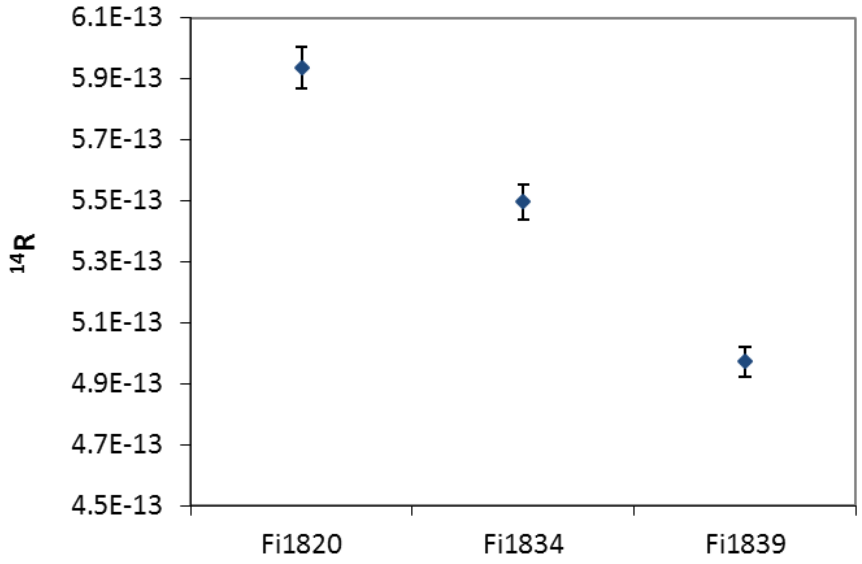

Figure 3.3 - $^{14}C/^{12}C$ isotopic ratios measured in secondary standard samples (IAEA C7) showing largely scattered values.

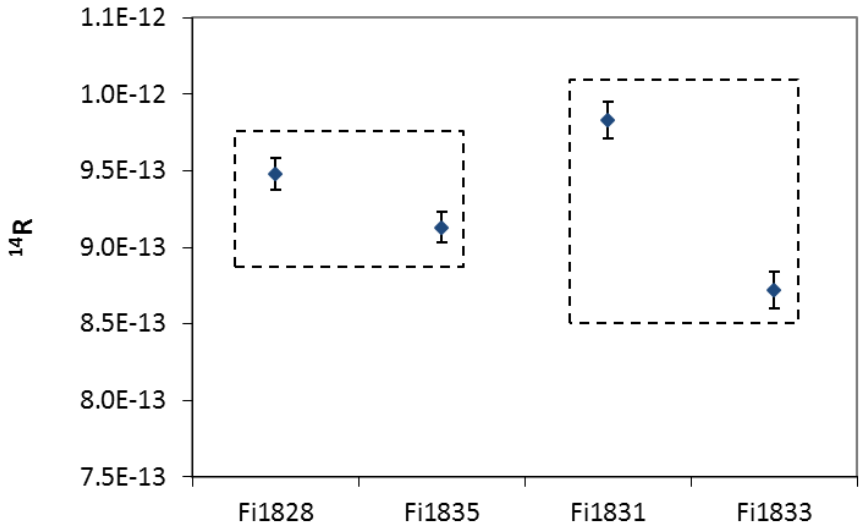

Figure 3.4 - $^{14}C/^{12}C$ isotopic ratios measured in unknown samples: each box identifies two fractions of the same sample. We obviously expected consistent values in each of the couples.

Huge contamination problems are evident. In particular, these data are explainable assuming that the contamination is caused by the sample burnt immediately before. Actually, with reference to Figure 3.3, for example, Fi1820 was burned after an Oxalic Acid II sample, and its concentration actually appears to be higher than the other IAEA C7 measured samples. If we check the Fi1834 sample, it was burned after a 350 years BP sample. Fi1839 was burned after a 10000 years BP sample, appearing to be the oldest among the shown three samples.

Applying a simple model, which accounts for the fact that the real radiocarbon concentration of each sample is contaminated by a given amount of the sample prepared immediately before, $^{14}R_{sample}$ can be expressed as:

$$^{14}R_{sample} = (1 + x)\ ^{14}R_{app} - x\ ^{14}R_c \qquad (3.1)$$

where $^{14}R_{app}$ is the measured apparent $^{14}C/^{12}C$ isotopic ratio, $^{14}R_c$ is the $^{14}C/^{12}C$ isotopic ratio of the contaminating sample, which contributes for a fraction x to the total mass of the sample.

Figures 3.5 shows the data corrected according to equation 3.1 for the same samples presented in figures 3.2, 3.3, 3.4. As a first approximation, a fraction of contamination x equal to 9.5% was used for all the samples. This fraction was chosen because it minimised the scattering among the Oxalic Acid II samples.

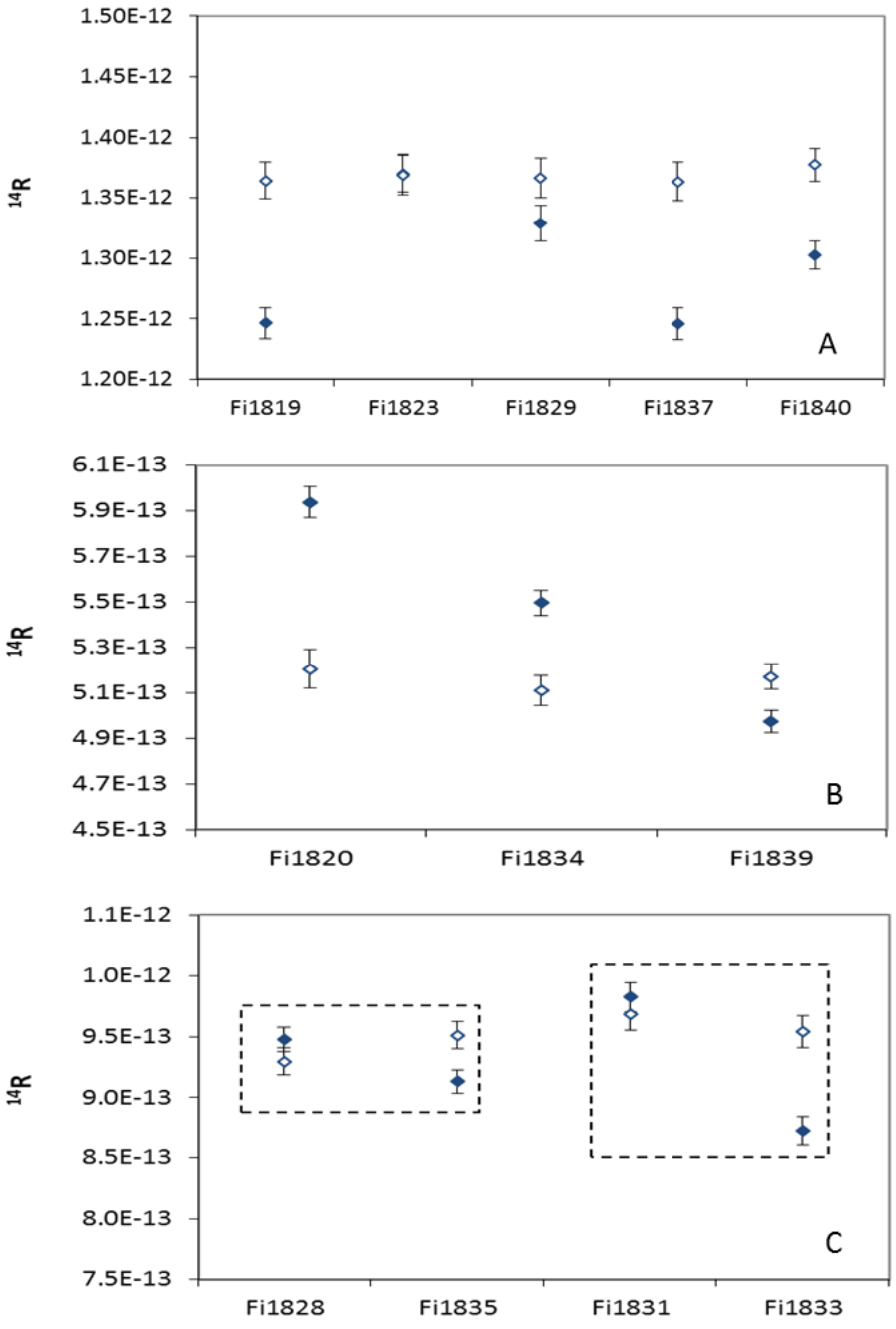

Figure 3.5 - $^{14}C/^{12}C$ isotopic ratios corrected (open diamond) applying the model of equation 3.3 for NIST Oxalic Acid II (A), IAEA C7 (B) and unknown samples (C).

o identify the source of the cross contamination, either the combustion or the graphitization process, the first step has been isolating the Elemental Analyser from the rest of the line. The EA was substituted with another instrument present at LABEC laboratory, indicated as new EA in table 3.1. Moreover, two samples were combusted in an independent setup, i.e. the oven of the preparation line dedicated to aerosol analysis (indicated as PM furnace in the table) [Cal2011]. For these two samples, CO_2 was trapped in an ampoule and then transferred to the graphitization line. For these measurements two kinds of blank samples were prepared: Cyclohexanone-2,4-DNPH (see paragraph 2.4) and graphite powder, high purity (Alfa Aesar pure graphite, 200 mesh).

Table 3.1 - Sequence of samples prepared to identify the source of memory effect. Some samples were burnt in the new EA, others in the combustion line dedicated to aerosol samples.

Lab code	Material	Combustion
Fi1943	NIST OxAcII	New EA
Fi1944	Blank (Alfa Aesar)	PM furnace
Fi1945	Blank (cyclohexanone)	New EA
Fi1946	Blank (Alfa Aesar)	PM furnace
Fi1947	Blank (cyclohexanone)	New EA
Fi1948	NIST OxAcII	New EA
Fi1949	Blank (cyclohexanone)	New EA
Fi1950	Blank (cyclohexanone)	New EA

The samples so prepared did not show any problem of cross contamination. In fact, the radiocarbon concentration measured in the samples prepared according to the sequence of table 3.1 were consistent with those expected. For instance, the ^{14}C measured concentration of blank samples Fi1949, burnt after Oxalic Acid Fi1948 in the new EA, is 0.50 ± 0.09 pMC, corresponding to an apparent conventional

radiocarbon age of about 42000 years BP. This test suggested that the "old" EA was the most probable source of memory effect.

Because of that, several parts of the EA were replaced. First of all, the gaschromatographic column was changed, but the following measurements on a sequence of samples of known ^{14}C concentration did not show any improvement. The role of the quartz combustion column was also investigated, even though it is usually kept at high temperature (900°C) and routinely changed and refilled with new chemical components[1]. Indeed, despite the replacement of reagents, any improvement was not detected in this case too.

Other two possible candidates to be responsible for the memory effect were the gas detector and the autosampler, because both are in contact with all samples. The focus was first on the autosampler, since replacing the gas detector would have been a quite expensive work.

Should the autosampler be the responsible of the cross contaminations, the principal cause would be the shaft inside, which is equipped with some seals that may break or may been damaged with operations. The shaft was replaced and another set of samples was prepared and measured. The results showed no more memory effect, but only small variations within the experimental uncertainty, as illustrated in figure 3.6.

[1] Usually, the replacement of material in the quartz column takes place when the combustions are not complete: in these cases, the acquired chromatograms show peaks even though any material is not inserted into the EA, as it is normally performed between two following samples.

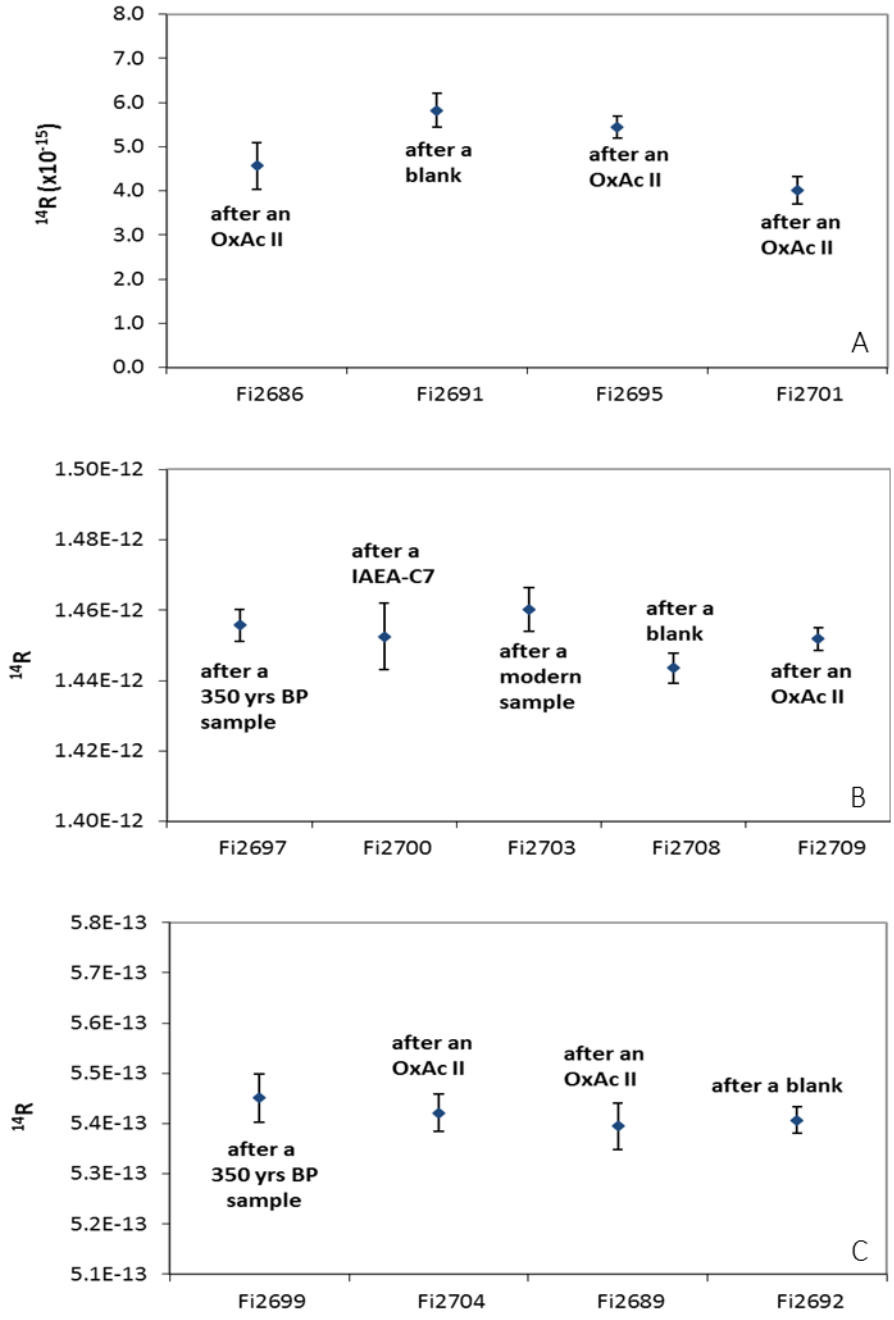

Figure 3.6 - $^{14}C/^{12}C$ isotopic ratios of blank (A), NIST Oxalic Acid II (B) and IAEA C7 (C) samples measured after replacing the shaft inside the autosampler. No memory effect is present, the small variations are within the experimental uncertainty.

In conclusion, this event of cross contamination was caused by a part of the autosampler [Fed2015].

3.1.2 New burning procedure using the elemental analyser

Following the memory effect episode, a new procedure concerning the combustion of the samples in the elemental analyser has been improved in order to minimize the risk of new contamination events.

Between two following samples, a blank combustion, i.e. a combustion without any kind of material in the EA, is performed. In this way we can check whether the combustion of the sample has been complete or not. In case of a complete reaction, we can reasonably assume that there are no residues in the quartz column.

In addition, before burning the "real" sample, a tiny fraction of the sample itself (typically ≤ 0.3 mg) is burnt. This precautionary combustion works to prevent that possible cross contamination due to first neighbours, as in the described case, may happen again. In fact, if the cross contamination occurs again, the contribution would be of the same radiocarbon concentration of the sample itself. In case the mass of the sample to be radiocarbon dated is not enough to guarantee at least one carbon pellet[2], we perform two blank combustions.

3.2 The case of restored samples by Paraloid B72

As already mentioned in paragraph 1.4, using synthetic products in the restoration field has become a very widespread habit. Among all possible materials, Paraloid B72®, also known as Acryloid B72®, is one of the most known. It has been employed since half of the last century, sold by Rohm and Haas Company. It consists in an acrylic resin formed by two polymers, ethyl methacrylate and methyl acrylate (EMA/MA) in proportion 70/30, shown in Figure 3.11.

[2] This can happen especially when dealing with bones whose collagen recovery yield can be very low.

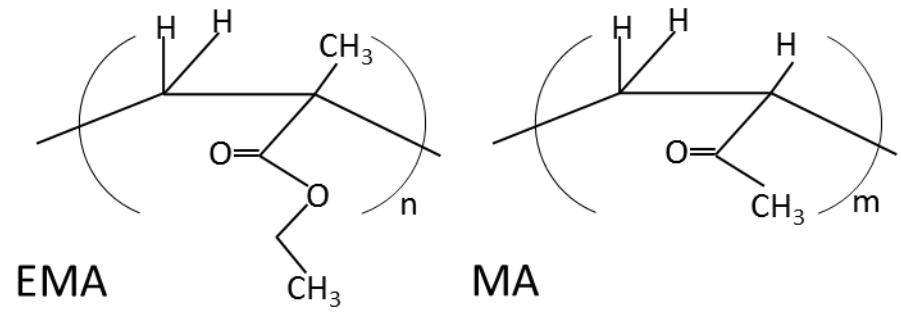

Figure 3.11 - The two monomers ethyl methacrylate (EMA) and methyl acrylate (MA), respectively, that constitute Paraloid B72.

Despite its level of diffusion, in the most recent years, the scientific community has focused on several problems about its use and removal. In fact, once Paraloid B72 is applied on an artwork, the removal process can be very difficult [Car2003]. It is well known that during the aging process of this acrylic resin, the physicochemical properties can change reducing solubility in the usual organic solvents. In principle, an effective removal may be obtained using solvents as chlorine-based products [Hor2010].

However, in the case of the removal of Paraloid during a restoration, using such pure solvents directly on the artworks is not feasible. In fact, the operator must avoid an uncontrolled dispersion of the solvent on the work, to prevent any damage to the work itself, and thus the solvents are frequently applied through a medium. Moreover, the removal is a mechanical operation that takes place layer by layer and may not enter deeply in the bulk. On the contrary, the removal of the contamination from a sample to be radiocarbon dated can be performed using a more aggressive solvent and the sample can be reduced in fragments to permit a better interaction. Of course, the removal has to be complete, from the surface to the bulk of the collected sample, to be really effective.

At the same time, any solvent or medium applied has to not leave any residue on the treated sample itself.

As mentioned, the issue of Paraloid removal is a greatly studied topic in scientific community [Caf2013, Car2008]. A first method for its removal is the use of the ultrasonic bath, once identified the solvent. However, the use of ultrasonic can stress and damage the sample itself, if the material is in a bad state of preservation [Ras2009]. In the literature, the most widely used extraction method for radiocarbon applications is based on the Soxhlet system [Bru2001], where the contaminated samples are treated with several organic solvents to remove contaminats. This procedure which involves the use of many solvents is effective, but it requires a full attendance of an operator. Another approach was developed over the last 20 years, i.e. new methodologies based on the development of nanoscience applied to Cultural Heritage [Bag2009]. The removal of acrylic resins by microemulsions applied using cellulose pulp o nanogels prove to be innovative and effective tools to cleaning painting surfaces, for example the frescos [Bag2014]. In the case of sample to be radiocarbon dated, the use of these sistems could involve the release of residues that can be potencial contaminats.

All considering, to find a simple way of operating, our choice to treat restored samples to be radiocarbon dated was focused on the use of a single solvent, not in the ultrasonic bath. Taking into account the properties of the chlorine-based compounds, chloroform ($CHCl_3$) was tested. This product is characterized by a great solvent power. In addition, one of its strong key points is its rapid evaporation and this is a very important requirement in order to exclude contamination effects due to the solvent itself. Of course, since chloroform is classified as harmful (Xn), irritant (Xi) and cancerogenic, it cannot be used without respecting any basic safety rules. The operator must use the right personal safety devices, wearing protective gloves, mask and goggles, and must work in a fume hood. When dealing with radiocarbon samples, this is the typical approach in case of the chemical pre-treatment.

3.3 The chloroform-based pre-treatment: preliminary results

The case study, which gave rise to research, was the wooden framework of the polyptic "Pala con la Vergine e il Bambino, S.Michele Arcangelo e Santi", an artwork by Ambrogio Lorenzetti (1290-1348 AD) painted in the first half of the 14th century. Two samples (OPD5 and OD7) were collected from the framework, attributed by the restorers to a period later than the painting (16th century). The wooden structure had been consolidated using Paraloid B72 and thus the collected samples were treated using chloroform as explained in the paragraph 3.2. As a comparison, a fraction of each of them was also treated following the only ABA procedure (see paragraph 2.2.1).

The chloroform-based procedure is developed according to the following steps:

- Cleaning the sample using tweezers and scalpel and reducing it into small fragments;
- Adding 5ml of chloroform per each 10 mg of sample in a close test tube at room temperature;
- Performing up to 4 extractions in 48 hours (while the tube is placed on a magnetic agitator);
- Drying the sample at room temperature under the fume hood for about 48 hours at least;
- Applying the ABA procedure.

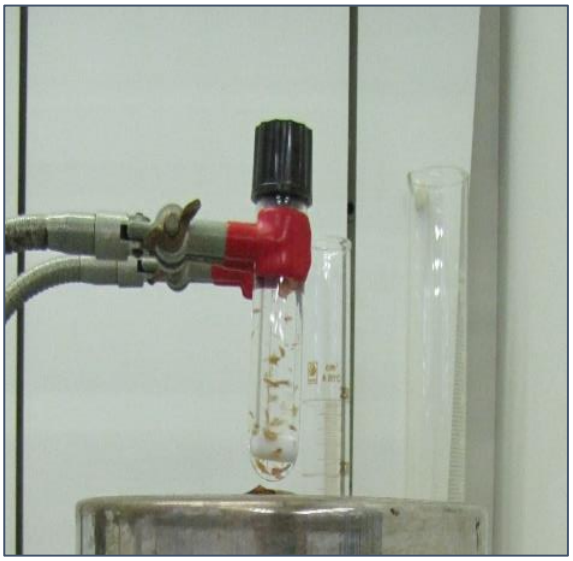

Figure 3.12 - Wooden chips are under agitation in the closed tube. The sample is soaked in chloroform to perform up to four extractions. The sample is reduced in small fragments permitting a better interaction with the solvent.

In table 3.2 radiocarbon data are summarised. In addition to the samples treated according to the whole procedure described above, for both OPD5 and OPD7, some wooden fragments were collected after each solvent extraction. Each time, on the collected wooden chips, ABA pre-treatment was applied for the AMS measurement.

Even though the real age of OPD5 and OPD7 is unknown (and can be only guessed on the basis of the restorers observations), in the case of the application of only ABA pre-treatment, the conventional radiocarbon ages t_{RC} do not appears realistic at all. They are not compatible with the expected value. In addition, the two samples are not consistent between each other. Another evidence that may suggest the presence of contamination is given by the uncertainty of OPD7 measured radiocarbon concentration. As mentioned, for each sample, two graphite pellets are usually prepared and measured: in the case of OPD7 pre-treated using only ABA procedure, the two measured fractions were very different one with respect the other. For this reason, the result is presented just using the simple average as the best estimate and

the maximum deviation as the error. These data can be explained with an incomplete removal of Paraloid.

Processing the fractions according to chloroform-based procedure, some removal of the contamination is visible already after the first extraction, even though it appears that four extractions are actually necessary to achieve a result that is consistent with the expected value. After the fourth extraction, OPD5 and OPD7 are also consistent between each other.

Table 3.2 - ^{14}C measured concentrations and corresponding radiocarbon ages for OPD5 and OPD7 samples pre-treated using the new chloroform-based procedure compared to only ABA method. These results confirm that in Paraloid contaminated samples, ABA is not sufficient to remove the resin. The removal of contamination is already visible after the first extraction, but up to four extractions are necessary to obtain an effective result.

	OPD5		OPD7	
SAMPLES	^{14}R (pMC)	t_{RC} (years BP)	^{14}R (pMC)	t_{RC} (years BP)
ABA only	77.90 ± 0.54	2005 ± 55	86.5 ± 1.2	1160 ± 110
1st extr.	93.92 ± 0.59	505 ± 50	94.20 ± 0.55	480 ± 50
2nd extr.	88.1 ± 1.6	1020 ± 145	94.6 ± 1.4	450 ± 120
3rd extr.	94.03 ± 0.77	495 ± 65	93.37 ± 0.73	550 ± 65
4th extr.	95.54 ± 0.49	370 ± 40	96.12 ± 0.49	320 ± 35

The same results are plotted in Figure 3.13 as the differences between the measured concentrations and the concentration measured after the fourth extraction.

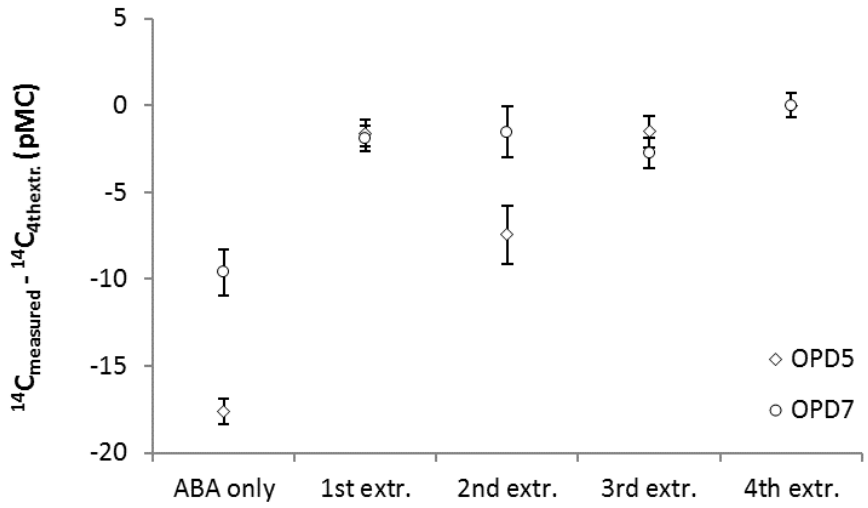

Figure 3.13 - ^{14}C concentrations in wooden samples taken from a historical restored artwork: the differences between measured values and the concentration measured after the 4th extraction in chloroform are plotted.

As it can be also noticed, the behaviour of the measured radiocarbon concentrations versus the number of extractions does not follow any significant trend. One could have supposed that the concentration increases as the number of extractions increases, with a trend roughly resembling an exponential curve. The measured behaviour can be explained considering a not homogenous distribution of Paraloid B72 in the wood during the restoration process, as it can be likely. The possible non-homogeneity may be due either to a gradient of penetration or to a different aging of the resin from the surface to the bulk.

Figures 3.14 and 3.15 show the calibrated ages for samples OPD5 and OPD7 at the end of the chloroform based-procedure: the data show that the ^{14}C concentrations measured after four extractions are consistent with what we could expect on the basis of the historical attribution given by the restorers.

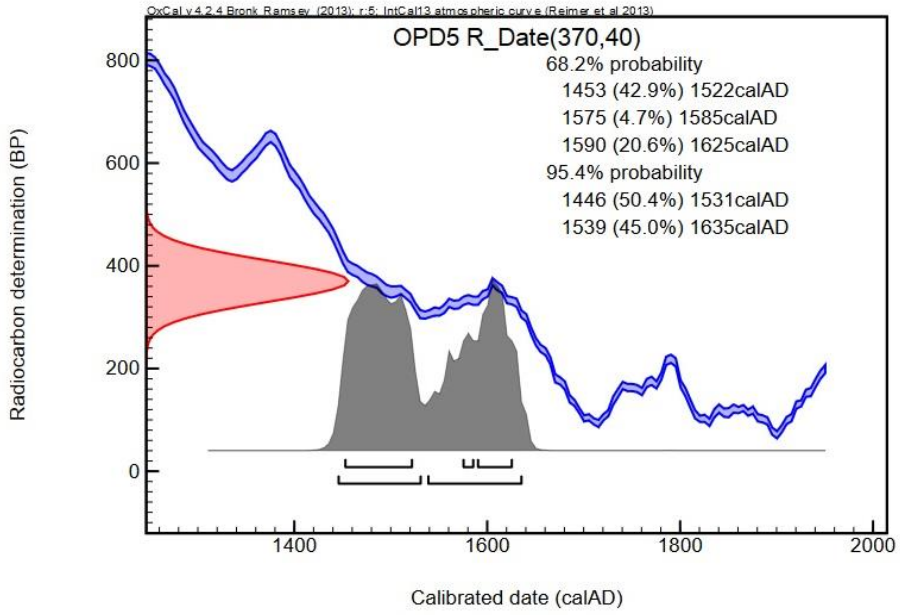

Figure 3.14 - Calibration of conventional radiocarbon age for OPD5 sample. Calibration software used is OxCal 4.2.

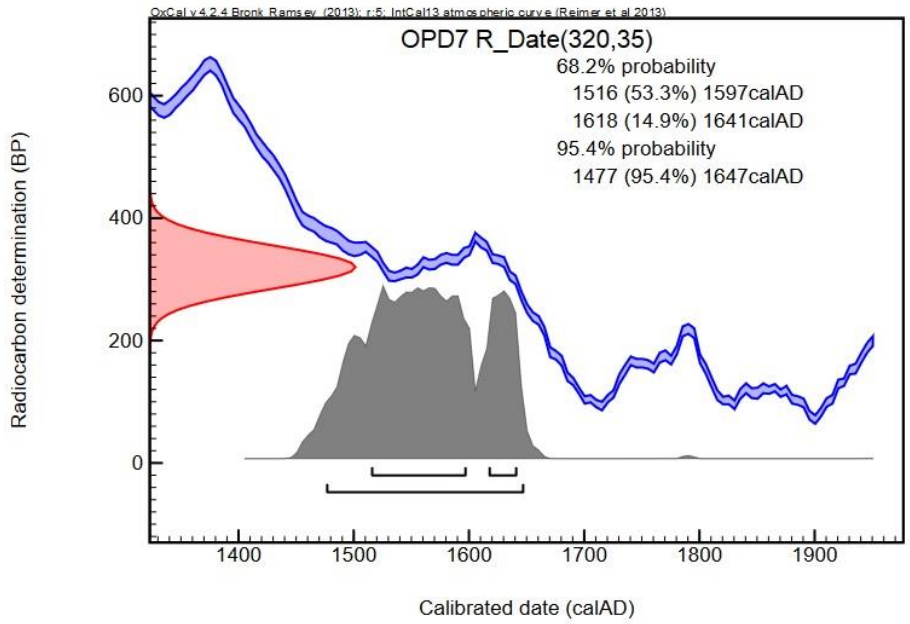

Figure 3.15 - Calibration of conventional radiocarbon age for OPD7 sample. Calibration software used is OxCal 4.2.

To better understand the effectiveness of chloroform-based procedure, this pre-treatment was applied to wooden test samples that were contaminated on purpose. These samples were analysed by FT-IR too, to study the possibility of using this technique to discriminate the presence of the contamination and to evaluate the effectiveness of its removal.

4. Restored wooden samples

The radiocarbon concentration measurements of the restored framework, discussed in chapter 3, clearly show us how the “dead carbon” contamination significantly ages the samples and how much efficient chloroform can be for its removal.

Wooden test sample were contaminated on purpose using Paraloid B72: AMS measurements were performed on wood fragments collected after each of the chloroform extractions to verify how the procedure was going on. Moreover, FT-IR spectra were acquired on wood and the liquid extracts to verify whether the sample pre-treatment has been successful

4.1 Test samples: oak and poplar wood naturally aged

In order to test the chloroform-based procedure, we chose oak (Quercus) and poplar (Populus) wooden samples taken from trees whose fell date was known.

The oak fragment was collected from a tree of about 80 years, cut in 2008, sampling it from the inner tree rings grown before 1945. In fact, since each tree ring “records” the radiocarbon concentration in atmosphere for each year of growth, in order to minimize possible differences among the measured ^{14}C concentration in contiguous fractions, the sample was collected where we could expect that the concentration does not change significantly from one ring to the other. As explained

in paragraph 1.2.2, in the so-called “modern” period (between about 1650 and 1950), the great quantity of CO_2 emitted by combustion of fossil fuels totally devoid of ^{14}C diluted the radiocarbon concentration in atmosphere (Suess effect). For the oak sample, we can thus expect to measure a radiocarbon concentration of about 97.8 pMC [Lev1989].

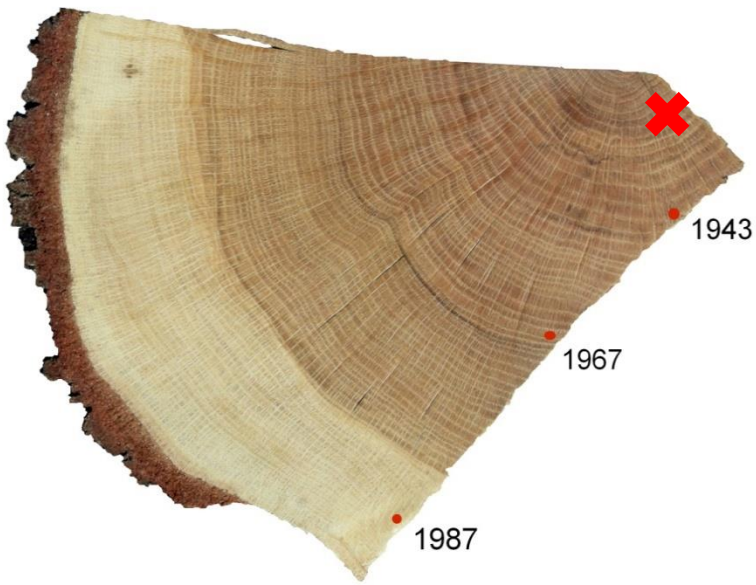

Figure 4.1 - Section of the oak tree taken for this study. The tree rings are well visible: the red cross corresponds to the area where the wooden fragment was collected for preparation of test samples.

The poplar fragment was collected from the most external ring of a tree cut in 2009, so that the radiocarbon concentration in atmosphere during 2009 can be considered as reference for the AMS measurements: the expected radiocarbon concentration is about 105 pMC [Hua2013].

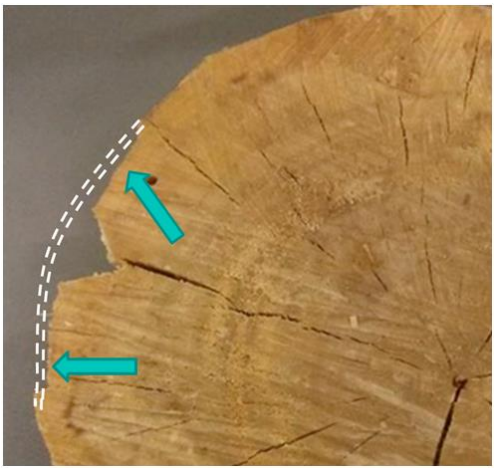

Figure 4.2 - Section of the poplar tree taken for this study. The tree rings are visible: the white dashed line corresponds to the collected area.

During my master degree (2011), the oak and poplar fragments were contaminated applying Paraloid B72 by brush [Lic2012; Fed2014]. Probably, the resin did not deeply penetrated into the wood structure, creating a film only on the surface. Since we know that the solubility of Paraloid B72 can decrease because of cross linking and time aging effects, we decided to measure the radiocarbon concentration processing the samples according to chloroform-based procedure after three years of natural aging in laboratory conditions. As shown in the case of OPD5 and OPD7 samples described in Chapter 3, we decided to measure the radiocarbon concentration not only at the end of the whole procedure, but also on some fractions of samples collected after each of the extractions.

In Table 4.1 the measured radiocarbon concentrations are shown.

Table 4.1 – Measured radiocarbon concentration in contaminated wooden fractions after each of the chloroform extractions.

SAMPLES	POPLAR	OAK
	^{14}R (pMC)	^{14}R (pMC)
Reference	104.31 ± 0.45	97.42 ± 0.33
ABA only	81.3 ± 2.1	88.94 ± 0.78
x_PARA_Chl1_ABA	103.71 ± 0.47	96.90 ± 0.61
x_PARA_Chl2_ABA	103.43 ± 0.43	97.05 ± 0.49
x_PARA_Chl3_ABA	103.66 ± 0.60	96.15 ± 0.71
x_PARA_Chl4_ABA	104.97 ± 0.72	98.00 ± 0.35

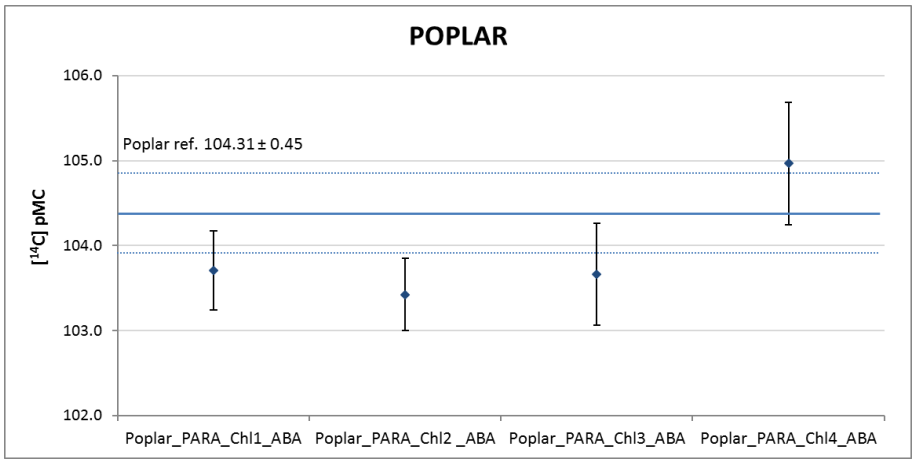

Figure 4.3 – Radiocarbon concentrations measured in the poplar sample as a function of the extractions number. The blue line indicates the radiocarbon concentration taken as reference.

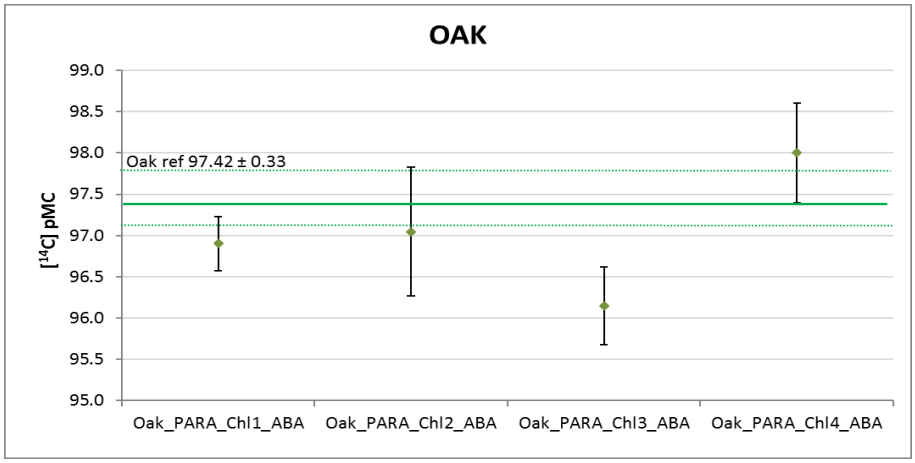

Figure 4.4 - Radiocarbon concentrations measured in the oak sample as a function of the extractions number. The green line indicates the radiocarbon concentration taken as reference.

Radiocarbon results are similar to those obtain for the OPD5 and OPD7 samples shown in chapter 3. Although it is clearly visible that the chloroform-based procedure is effective for these samples, the dependence with the number of extractions is not so clear. We expected that the measured ^{14}C concentration could approach to the reference value increasing the number of extraction. Instead, the data do not show any evident trend. In both cases, already after the first solvent extraction, the measured radiocarbon concentration is consistent with the expected value. If a contamination is still present after the first extraction, its contribution to the measured radiocarbon concentration is however within the experimental uncertainty. Such a result can be interpreted supposing that the three years of natural aging have not been enough to age the resin in a very important way. The solubility properties of the product may have not severely changed.

Moreover, some fractions show quite surprising results: for instance, the concentration for Oak_PARA_Chl3_ABA sample has been measured to be lower than the concentration measured for Oak_PARA_Chl2_ABA. This “strange” behaviour can be explained considering the possible non-homogeneity of the distribution of Paraloid inside the samples. Actually, Paraloid B72 was applied on the test samples by brush as a thin layer and it might have not deeply penetrated in the wood structure.

These preliminary tests show us that the use of only radiocarbon dating to investigate the behaviour of Paraloid removing is not sufficient. The possibility to apply another technique can be useful to better understand the process. For this reason, FT-IR technique has been investigated as a complementary method.

4.2 Test samples: poplar wood artificially aged

New wooden test samples were prepared from the same poplar tree ring. In order to facilitate a homogenous distribution of Paraloid B72 in the whole samples, a special attention was payed when cutting the wood. The fragments were collected so that their thickness was small enough to allow the resin to penetrate as much homogeneously as possible. Therefore, a syringe was used instead of a brush to apply Paraloid. Indeed, together with the brush and the spray methods, the use of a syringe to inject a resin for consolidation purposes is a method employed by the restorers themselves, especially in the case of point-like operations. Different volumes of acrylic resin were injected in the samples to understand if the removal of Paraloid B72 can depend on the mass present in the material. Before any measurement, the test samples were artificially aged.

AMS measurements (following the only ABA treatment) and FTIR analyses were performed on the contaminated aged samples in order to characterize the "state of the art" of the samples. In addition, the chloroform pre-treatment was applied: for each of the four extractions, we performed a FTIR measurement on the extracts (collected after the evaporation of the solvent) and an AMS measurement on the wood fragment, in order to verify how the procedure was going on.

4.2.1 Characterization of the applied Paraloid B72

To contaminate the samples, a solution of Paraloid B72 and acetone was prepared. Indeed, as it is typically available on the market, Paraloid B72 is not ready to use: it is

sold in the form of pellets that have to be dissolved in a solvent such as typically ethanol, acetone or butyl acetate. In our case, we chose acetone, which is one of the most common solvent in the artworks restoration field [Koob1986]. The solution was prepared according to a volume ratio of acetone versus Paraloid pellet of 90:10.

After the solvent evaporation, as a common sample to be radiocarbon dated, a portion of Paraloid B72 film was collected and measured by AMS. The two prepared pellets Fi3123 and Fi3127 (see Table 4.2) were consistent, so the weighted average was determined as the best estimate of Paraloid B72 radiocarbon concentration: 20.96 ± 0.16 pMC.

Table 4.2– Measured radiocarbon concentration in the Paraloid B72 sample.

Samples	^{14}R (pMC)	t_{RC} (years BP)
Fi3123	20.72 ± 0.20	12645 ± 80
Fi3127	21.34 ± 0.25	12410 ± 95
Paraloid B72	20.96 ± 0.16	12550 ± 60

This result partly surprised us, since we had expected a lower concentration, i.e. a concentration roughly of the same order of magnitude of the one of the blank samples (typically about 0.4 pMC). However, it is clear that such an "old" resin strongly contributes to dilute the sample radiocarbon concentration, aging the sample to be dated if not completely removed.

Figure 4.5 shows the FTIR spectrum[1] acquired on a drop of the Paraloid solution after acetone evaporation.

In the spectrum, characteristic bands are well recognizable. The bands around 3000-2900 cm^{-1} are due to C-H stretching bond. The band around 1740 cm^{-1} is due to

[1] All the spectra shown in this work are acquired using Shimadzu FTIR-8400S spectrometer with a resolution of 2.0cm^{-1} and 16 scans per sample.

C=O stretching bond of the ester group of monomeric units derived from methyl acrylate and methyl methacrylate that constitute Paraloid B72 [Der1999]. Others bands fall in the so-called fingerprint region, which is really peculiar for each material, but it can be strongly modified by the interference of other compounds in the same sample (e.g see the C-H bending bond at ~1475-1445 $cm^{-1}$and 1385-1365 cm^{-1}, the C-O stretching bond in the range 1265-1145 cm^{-1} and at~1025 cm^{-1}).

These functional groups are present in most of the materials and thus the corresponding absorption peaks may not be so helpful for the discrimination of the resin with respect to the possible substrate, e.g. wood, as in our case. The most easily recognizable band, well separated from the others, that can be proposed as the reference marker for our case appears to be the one around 1740 cm^{-1}.

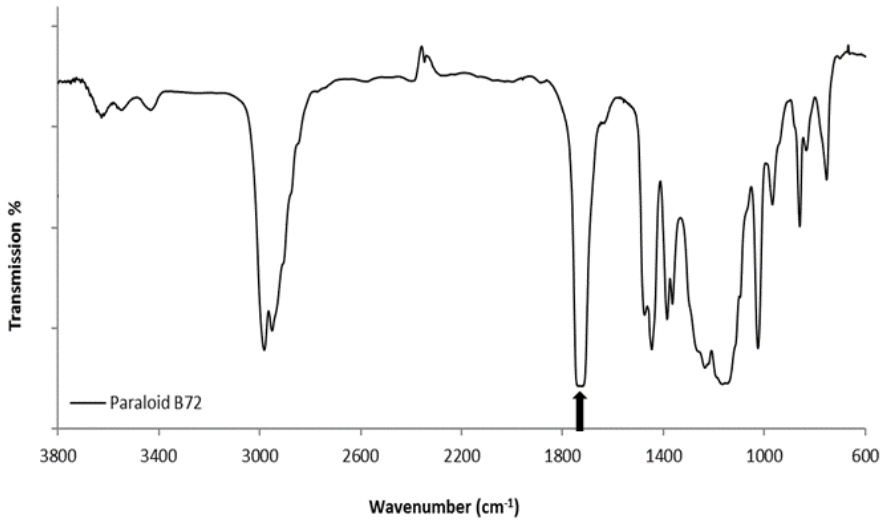

Figure 4.5 – FT-IR spectrum of Paraloid B72 obtained after evaporation of the solvent (acetone). The most easily recognizable band is around 1740 cm^{-1}: this is due to the C=O stretching bond of the ester group (see the arrow in the graph). Other low-intensity bands not ascribable to Paraloid are also present: in the region 3600-3400 cm^{-1}they are due to O-H stretching and can be attributed to possible residual traces of acetone; in the region 2350-2330 cm^{-1}, they can be explained considering residual atmospheric carbon dioxide.

4.2.2 Preparation of test samples: contamination and artificial aging

From the portion of the cut tree ring, three thin slices of wood (about 20x10x1mm^3) were carefully cut.

Different volumes of solution Paraloid B72/acetone, i.e.0.15, 0.30 and 0.50 ml, were injected using a syringe to be sure that the consolidant has penetrated in the wood and that it was not present only as a surface layer. In the following, these test samples are referred to as Poplar0.15, Poplar0.30 and Poplar0.50, respectively.

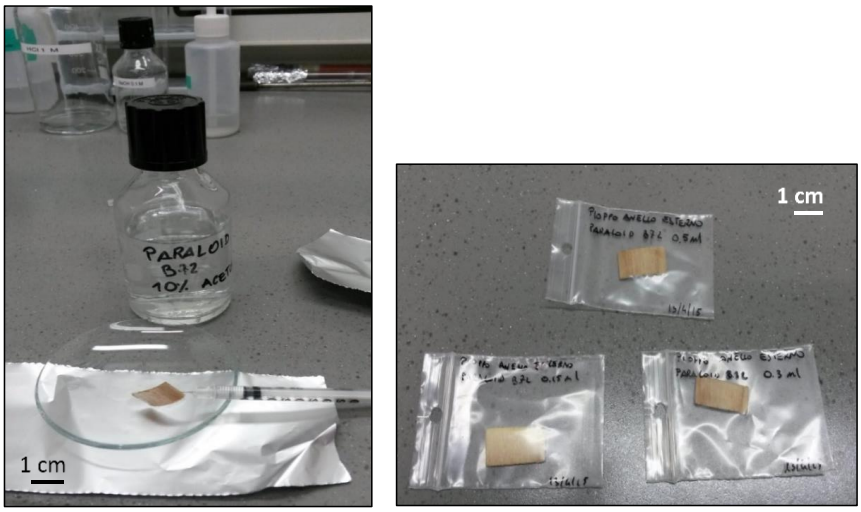

Figure 4.6 – The wooden test samples. Different volumes of Paraloid B72 were injected into the wood using a syringe.

Once contaminated, a key step in the study was represented by the aging of the samples. Actually, reproducing the natural conditions of light, temperature and humidity in an artificial aging is not straightforward. To simulate in a reasonable short period what can naturally occurs during longer times, we can typically use a climatic chamber, in which we can control temperature and irradiation conditions so as to simulate natural environmental effects[2] [Chi2001, Cap2012]. The role of the

[2] Some models of climatic chamber allow us also to control the relative humidity.

temperature in degradation process is represented by the fact that the kinetic reaction rate increases, while the wavelength of the irradiation source contributes to photooxidation: the energy of radiation is sufficient to break polymeric bonds. However, replicating all the natural photochemical processes that produce the deterioration in materials such as paint, varnishes and wood can be highly complex to know in advance [Fel1994].

In this work, we used a CO.FO.ME.GRA Solarbox3000. This device is equipped with a 550 W/m^2 Xenon lamp and a UV filter, cutting the radiation components characterized by a wavelength $\lambda < 290$ nm, to simulate outdoor exposure. The radiant heat produced by the Xenon lamp is continuously monitored and controlled by a black standard thermometer (BST), which is placed in the same plane where the samples are allocated.

The three test samples (Poplar0.15, Poplar0.30 and Poplar0.50) were irradiated in the climatic chamber for about 500 hours, at a temperature of 60°C.

4.2.3 AMS measurements

At the end of the aging period, each of the samples Poplar0.15, Poplar0.30 and Poplar0.50 was divided into two subsets: one part was collected for only ABA pre-treatment, the other was collected for the chloroform-based process (see paragraph 3.3).

As already discussed for the other wooden samples of this study, after each extraction in chloroform, some fragments of the treated sample and the liquid extracts (mixture of chloroform and possible removed Paraloid B72) were collected for AMS radiocarbon and FT-IR analyses, respectively.

AMS results are summarised in table 4.3.

Table 4.3 - Measured ^{14}C concentrations of wooden test samples. Uncertainties are quoted at 1 sigma level. The reference ^{14}C concentration for poplar was measured as 104.31±0.45 pMC [Fed2014].

	Poplar0.15	**Poplar0.30**	**Poplar0.50**
	^{14}R (pMC)	**^{14}R** (pMC)	**^{14}R** (pMC)
ABA only	90.55 ± 0.88	74.1 ± 1.4	78.7 ± 2.5
1st extr.	103.71 ± 0.43	102.83 ± 0.54	103.31 ± 0.67
2nd extr.	102.55 ± 0.53	102.84 ± 0.37	104.32 ± 0.38
3rd extr.	104.04 ± 0.45	102.90 ± 0.66	103.59 ± 0.42
4th extr.	103.27 ± 0.47	103.29 ± 0.42	103.49 ± 0.52

The radiocarbon data are also shown in figure 4.7, plotted as the differences between the measured concentrations and the reference poplar concentration (104.31 ±0.45 pMC [Fed2014]).

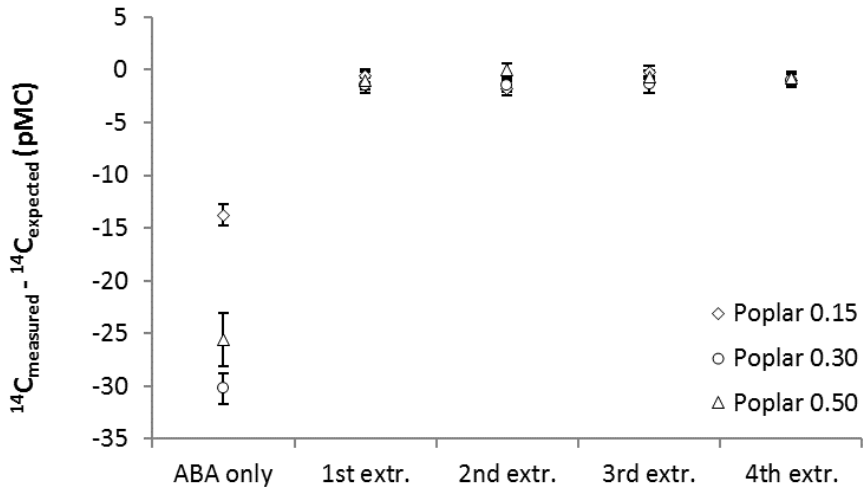

Figure 4.7 - ^{14}C concentrations in the wood test samples contaminated with different volumes of Paraloid B72 (0.15 ml, 0.30 ml and 0.50 ml): the differences between measured values and the reference poplar concentration are plotted.

As we expected and as the already measured samples has also shown, it is clear that the simple ABA pre-treatment is not sufficient to remove the contamination due to the synthetic resin.

The efficiency of chloroform is evident, as it is also foreseen too. Data show that, already after the first extraction, measured radiocarbon concentrations are approaching the expected value, independently from the amount of the added Paraloid. After the third and the fourth extractions, all the measured concentrations are consistent with the expected value within 2 sigmas.

Radiocarbon results also suggest that the effect of the contamination and the easiness of its removal do not appear to be dependent on the applied volume of Paraloid B72. This may be explained by considering a non-homogeneous distribution of the resin inside the samples, although we payed attention to the injection of the contaminant. We may also assume that the artificial aging performed has not significantly changed the solubility of Paraloid. It is in fact probable that the contamination effect and thus the possible difficulty of its removal are more dependent on the state of preservation of Paraloid rather than on its volume.

4.2.4 FT-IR analyses

FT-IR spectra were acquired on Poplar0.15, Poplar0.30 and Poplar0.50 to characterise the presence of Paraloid B72, comparing them to raw poplar.

Using a scalpel, as small as possible chips were cut from the slices of wood described in paragraph 4.2.2. By mixing the wooden small fragments (about 1mg of wood chips) with KBr powder, obtaining uniform pellets is very difficult. Thus, the possibility that the IR adsorption is not homogenous all over the whole surface cannot be neglected. This occurrence can influence especially the fingerprint region, but also the intensity of the other bands. In figure 4.8, the FT-IR spectra acquired on raw poplar sample and on contaminated poplar samples are presented.

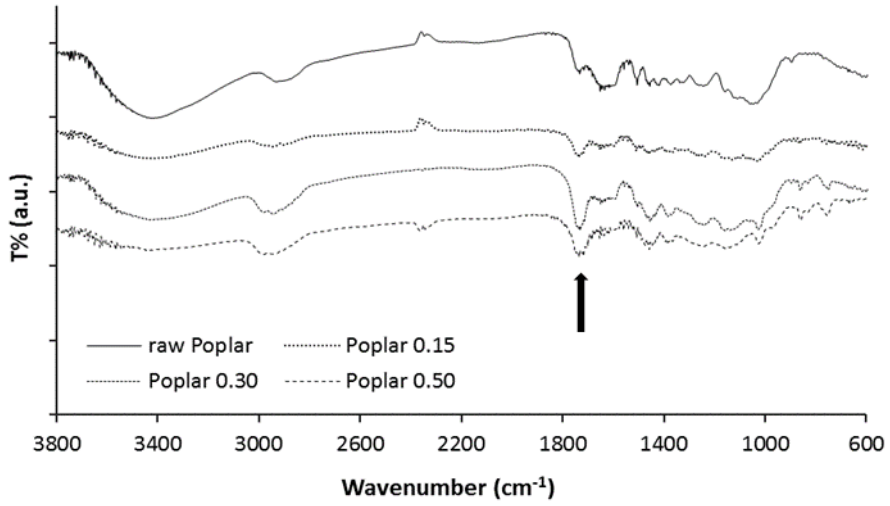

Figure 4.8 – FT-IR spectra of the test samples collected from poplar: raw (Poplar) and contaminated (Poplar 0.15, Poplar 0.30 and Poplar 0.50). The band around 1740 cm^{-1} (see the arrow in the graph) can be considered as a marker of the contamination due to Paraloid B72.

Observing the spectra, only qualitative interpretation can be drawn.

A first consideration is about the real great difficulty to prepare homogeneous and reasonably transparent KBr pellets starting from such small quantities of wood. Obviously, we might have prepared a bigger sample, achieving the powder to be pressed in the KBr pellet by grinding the wood using a typical milling machine. Anyway, we decided to work in the "normal" conditions that are characteristics of radiocarbon measurements on wood: in these cases, the collected masses are effectively small, typically few mg.

The reference band at about 1740 cm^{-1} (see the arrow in the graph) is visible in all samples, in the raw wood spectrum too. In the raw poplar, the band is due to the same ester groups that are present in the wood structure. However, it is possible to observe that this band is clearly more noticeable when Paraloid B72 is applied and it basically increases as the contamination itself increases, even though a direct proportionality cannot be found.

The use of FT-IR as a tool for preliminary investigation on the contaminated samples can give us only qualitative information about the presence of Paraloid B72,

but it cannot answer to the question whether how much contamination is present.

New and different information can be achieved acquiring FT-IR spectra on the liquid extracts collected during the chloroform-based procedure.

In principle, each collected extract could contain Paraloid B72, but in a very diluted state. Thus, just depositing the solution on the KBr plate does not give any useful indications. So, each liquid sample was first dried in a rotary evaporator to remove the chloroform itself, and eventually the residues were deposited on KBr plate in order to permit the analysis.

The acquired FT-IR spectra are shown in Figure 4.9. For all the poplar samples, an intense band around 1740 cm^{-1} is present in the spectra acquired after the first and the second extraction, while in the spectra acquired after the third and the fourth extraction, this band cannot be discriminated with respect to the background noise.

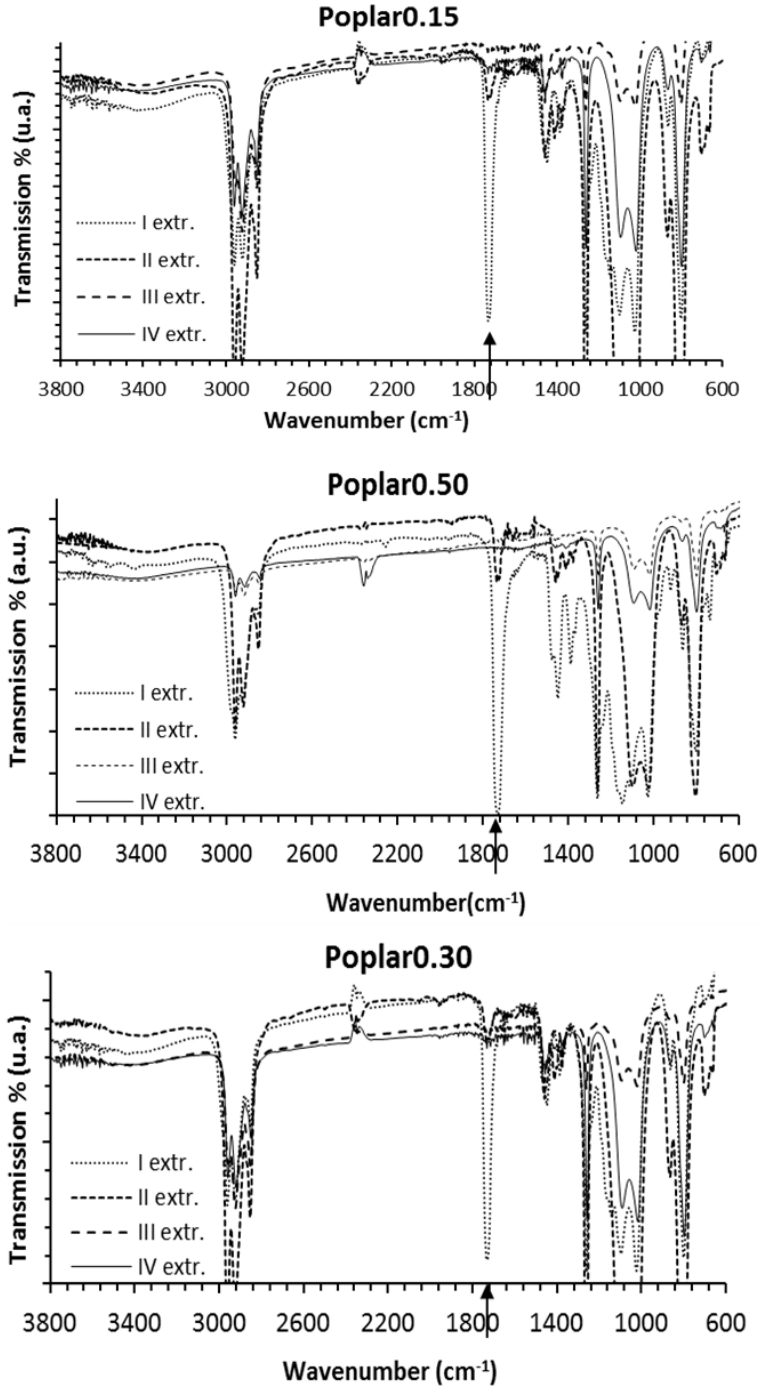

Figure 4.9 - Spectra acquired on the collected liquid extracts while processing the Poplar0.15, Poplar0.30 and Poplar0.50 samples. The band around 1740 cm^{-1} is very clear in the spectra acquired after the first and the second extraction in all the analysed samples.

In the analysed extracts, the band at 1740cm^{-1} is not visible starting from the third extract. This seems to confirm that the first two extractions are enough to remove the contamination due to Paraloid B72.

Another brief comment on the FT-IR spectra is also relevant. Together with the decrease of the band at 1740cm^{-1}, we could expect also the decrease of the other bands that characterise the Paraloid spectrum, such as the bands around 2900 cm^{-1} and the bands present in the fingerprint region. On the contrary, this does not happen and especially the fingerprint region is marked by several very intense peaks. We can explain the presence of these bands as interferences due to some silicone oils present in the syringes which were used to collect the extracts and were actually partially dissolved by chloroform.

The measured ^{14}C concentration on the fragments after the chloroform extractions are consistent with the interpretation of FT-IR spectra. In the third extract, the band at 1740 cm^{-1} is not clearly visible and in fact the radiocarbon concentration measured in the associated wooden fraction is compatible with the expected value within 2 sigmas, as already discussed in paragraph 4.2.3. The two different techniques, ^{14}C-AMS and FT-IR applied on the extracts, can be used in this case as complementary methods, considering that one is a sort of photographic negative of the other.

Therefore, the possibility of closely check the effectiveness of the extraction could be a useful monitoring procedure to be introduced routinely during the sample pre-treatment steps.

5.Restored bone samples

The chloroform-based procedure, discussed in paragraph 3.3, was tested on osteological remains collected from the Anthropological Museum collection of University of Florence, where Paraloid B72 is used to restore the broken bones. Moreover, the chloroform-based procedure was applied on consolidated bone samples collected during an archaeological survey in the south of Cyprus island.

5.1 Characteristics of bone samples

In archaeology and history, the study of bone remains permits to acquire information about processes associated with life of human groups, e.g. the state of health and the relationship between individuals, or simply the evolution during centuries. In particular, the possibility of radiocarbon dating bone samples is very useful for the archaeologists. Indeed, dating bones “takes a picture” of really what we are interested in, i.e. the moment of the organism death. Bones can be also used for stable isotope analysis in case of studies about diet and origin of populations.

In a vertebrate organism, the set of bones constitutes the skeleton. It is well known that the skeleton supports several important roles as sustain and protection of soft tissues, production of red and white blood cells (in the bone

marrow) and storage of minerals. Obviously, bones permit also the mobility acting as a support for the body as insertion sites for tendons and ligaments. According to their structure, bones can be divided into spongy or compact, and according to their form, they can be divided into long, short or flat.

In a living organism, a bone is typically formed for about 10% of water, for about 20-30% of organic fraction and for about 60-70% of inorganic phase [Rei2002]. The latter is formed by carbonate and calcium fluoride, magnesium phosphate and mainly by non-stoichiometric hydroxyapatite $Ca_{10}(PO_4)_6(OH)_2$. In a burial context, this mineral composition is subjected to modification by substitution of phosphate with the carbonate groups.

The organic fraction is mainly constituted by collagen. Basically, collagen is a fibrous protein composed by three polypeptide chains that wrap each other with spiral-shaped conformation (collagen fibrils). These structures are associated to form collagen fibres [Hau1972].

In theory, both the mineral phase and the collagen can be used for radiocarbon dating. However, buried bones can be subjected to diagenesis processes[1]. Since the dissolution processes take place in contact with the soil, the mineral fraction appears more sensitive to isotopic exchanges with respect to the organic one and therefore it is more subjected to contaminations with exogenous carbon. Basically, the collagen is thus the suitable fraction to be dated.

The possible diagenesis causes have not been well understood yet because they are very complex. The involved variables are several and they principally depend on conservation conditions, on composition of soil and on climate. In fact, high temperatures, humid environments and low pH level of soil contribute to accelerate the degradation processes. The diagenesis entails also to the loss of collagen. In general, the loss of collagen is slower in temperate climate environments than in environments characterised by warmer temperature and frequent rainfalls (subtropical

[1] With the term diagenesis, all the events that cause the degradation of the whole bone are typically referred to.

climate) where the loss of collagen is more accelerated. Basically, if the loss of collagen is high, the probability of that the residual collagen is contaminated, increases.

Thus, in general, when dealing with the extraction of collagen from an archaeological bone, what can happen is:

- Collagen presents a huge contamination and does not provide any useful information;
- The bone is so much degraded that there is no more collagen in the sample.

In both cases, the radiocarbon measurement has basically no sense.

5.2 Bone samples pre-treatment: the collagen extraction

Typically, in a sufficiently well-preserved bone collected in an archaeological site, the residual collagen is between 1% and 5%. For this reason, the minimum mass required to perform the radiocarbon pre-treatment is about 500 mg at least.

As already introduced in the previous paragraph, the aim of bone samples pre-treatment is at extracting collagen. The first step is the removal of the most external layers through a mechanical cleaning as described in paragraph 2.2.1. Then the samples are ground in a mortar to facilitate the successive chemical attack. The chemical pre-treatment is performed following a modified procedure derived from the Longin method [Lon1971]:

- Complete demineralization in aqueous HCl at room temperature for about 24 hours, at least;
- Purification in aqueous 0.1M NaOH at room temperature for 2 hours;
- Further bath in 1M HCl at room temperature for 2 hours to remove any CO_2 possibly absorbed from atmosphere during the second step;
- Gelatinization of the collagen-based acidified solution (pH ~3) at 80°C.

Usually, the concentration of acidic solution during the first step is 0.5 M, but if the bone sample is suspected to present a great degradation, a gentler acidic solution is used. In this case, the duration of the demineralization step can be even more than 24 hours. Obviously, the HCl solution is frequently changed to improve the efficiency of reaction [Sci2013].

5.2.1 C/N atomic ratio as a collagen quality indicator

Considering the diagenesis, i.e. all those processes that involve the degradation to bone, once completed the extraction procedure - actually if collagen is present – investigating the state of preservation and the presence of possible contaminants is of crucial importance.

There are some collagen quality indicators that can be used to define the different state of collagen preservation through different analytical techniques, such as the characterisation of amino acid composition [Klin1999]. Among these, a useful indication can be given by carbon/nitrogen atomic ratio (C/N). This is an "easy" measurement that does not require an extra amount of sample because the C/N ratio can be obtained during the sample combustion in the elemental analyser (see paragraph 2.2.2). In the literature, a suitable value of C/N ratio is reported as between 2.9 and 3.6. In this range, collagen is considered in a good preservation state [DeN1985]. Lower values are usually due to the presence of inorganic compounds, whereas higher values are due to the presence of exogenous organic carbon.

5.3 The chloroform-based procedure applied to restored bones

When bones to be radiocarbon dated are not directly recovered from an archaeological site but are collected from a museum context, it may be necessary to pay attention to the possible presence of restorations as for any other material.

The resin Paraloid B72 is also commonly used in the restoration of broken bones as a glue [Koo1986]. As in the case of wooden sample (paragraph 3.3), a partial removal of this synthetic resin involves a lower measured radiocarbon concentration, therefore an apparent aging can affect the bone sample dating.

The chloroform-based treatment already described in paragraph 3.3 has been also applied to such contaminated bone samples. Processing these samples, the chloroform is added before extracting collagen. Following an outline of the procedure:

- Mechanical cleaning and grinding in mortar of the sample;
- Adding chloroform to bone powder in a close tube, located on a magnetic agitator;
- Performing up to 4 extractions in 48 hours;
- Drying the sample at room temperature under the fume hood for about 48 hours;
- Applying the modified Longin procedure to extract the collagen, as already described in paragraph 5.2.

5.3.1 Preliminary investigations

As a first step, some preliminary measurements were performed on an archaeological bone that had not been consolidated to investigate whether the chloroform-based procedure could degrade the collagen.

One portion of bone powder (Bone_Long) was pre-treated using the usual procedure to extract collagen, as described in paragraph 5.2. The residual sample (Bone_Chl_Long) was pre-treated according to the chloroform-based procedure. In the case of the fraction Bone_Long, the extracted collagen was not sufficient to prepare two distinct pellets for the measurement (laboratory code Fi3044). Instead, in the case of the sample pre-treated using the chloroform-based procedure, the extract collagen was enough to prepare two pellets (Fi3043 and Fi3047).

As it is possible to observe in figure 5.1, the pellets Fi3043 and Fi3047, as well as being consistent between each other, are also consistent with Fi3044.

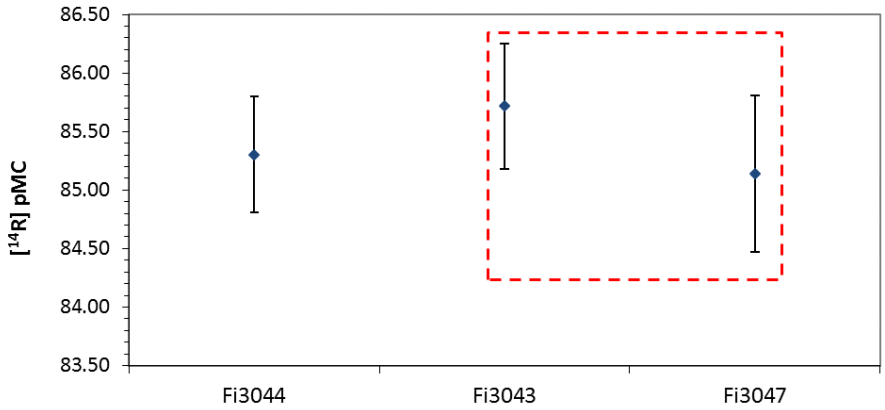

Figure 5.1 – The pellet Fi3043 and Fi3047are consistent between each other (treated according to the chloroform-based procedure) and they are also consistent with Fi3044 (prepared according the Longin modified procedure).

In Table 5.1, the results are summarised. In the case of Bone_Chl_Long, the best estimate of ^{14}C concentration is evaluated as the weighted average of the two measured concentrations.

Table 5.1 – Measured radiocarbon concentrations in a not-consolidated bone. One fraction of the sample was pre-treated using only the modified Longin procedure, the other was processed adding the chloroform before collagen extraction.

SAMPLES	^{14}R (pMC)
Bone_Long	85.30 ± 0.50
Bone_Chl_Long	85.49 ± 0.42

These results suggest us that chloroform does not degrade the collagen present in the bone sample to be radiocarbon dated, as we recovered good collagen in the chloroform treated sample as well. In addition, we can observe that the solvent do not leave any residue (or contamination) on the treated sample, being the two measured fractions consistent.

5.4 Bones from medieval period

The bones used to investigate the effectiveness of the chloroform-based procedure were collected in the archaeological area of Porticus Octaviae in Rome and they were restored on behalf of Anthropological Museum of the University of Florence.

Porticus Octaviae is a very complex archaeological area dedicated to worship since its foundation. The archaeologists have identified several phases of construction starting from the first building erected in 146 BC. At the present moment, the visible architectures are attributed to a period around 200 AD. In the Middle Ages, the same spaces were used to build a church with a great beside cemetery. The latter has been used for about three centuries for burials that were located on different levels until the full abandonment of the area around the 13^{th} century [Cia2009].

An ulna and an humerus were chosen for this study because these bones had been restored using Paraloid as a glue. In fact, many of the osteological remains found in the burials present fractures: the broken bones are usually glued to study the shape, length and characteristics of the bone. In figure 5.2, the areas where the samples were collected from are shown. Four samples were collected from each of the bones: three of them from the resin-glued break, clearly expected to be contaminated, and the other from one of the bone extremes, far from the break. We expected that this one is not contaminated and thus its measured radiocarbon concentration has been used as reference.

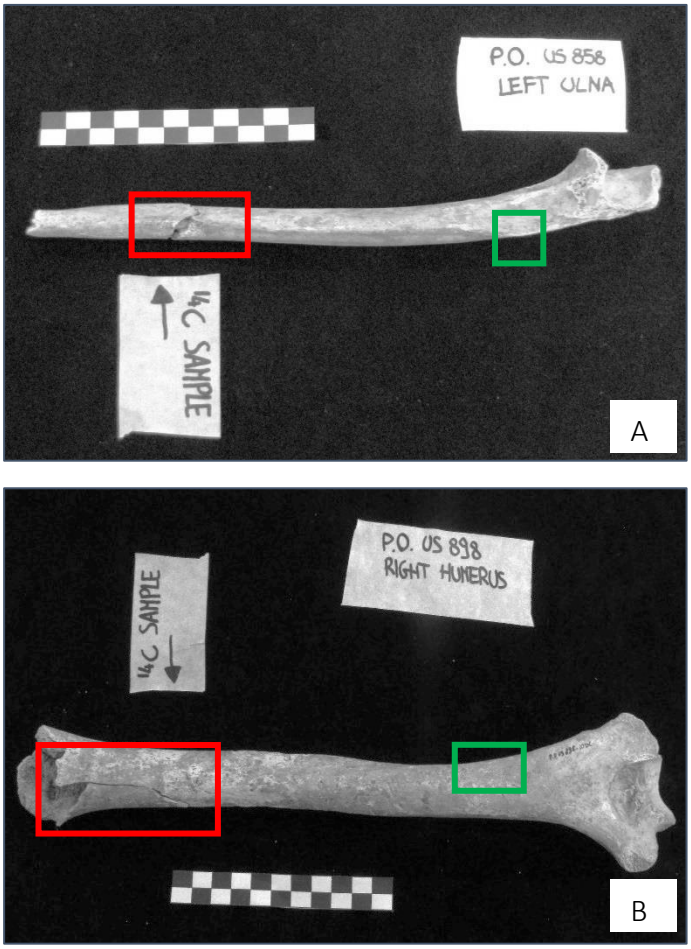

Figure 5.2 - The ulna (A) and humerus (B) bones chosen for this study: the green box indicates the clean area where the sample used as reference was collected; the red one indicates the restored area where the collected samples are expected to be contaminated by the applied Paraloid.

The samples collected in the clean area were pre-treated according to the "usual" procedure (see paragraph 5.2). The samples collected in the Paraloid B72 contaminated area were pre-treated using two different procedures. One part was processed without taking the possibility of contamination into account, while the other two fragments were processed using the chloroform-based pre-treatment[2]. In table 5.2 all the samples are summarised.

[2]We processed two distinct contaminated samples for each bone (x_PARA_Chl_LON in the text) to check the reproducibility of the effectiveness of the chloroform-based process.

Table 5.2– Scheme of the samples with the respective pre-treatments.

SAMPLES	STATE OF THE SAMPLES	PROCEDURE
ULNA_ref	Uncontaminated	mod. Longin
ULNA_PARA_LON	Contaminated	mod. Longin
ULNA_PARA_Chl_LON (x2)	Contaminated	Chloroform + mod. Longin
HUMERUS_ref	Uncontaminated	mod. Longin
HUMERUS_PARA_LON	Contaminated	mod. Longin
HUMERUS_PARA_Chl_LON (x2)	Contaminated	Chloroform + mod. Longin

5.4.1 C/N ratio measurements

The samples were pre-treated according to the procedure reported in table 5.2, then they were combusted in the elemental analyser (see paragraph 2.2.2). During this phase, the CO_2 is separated from the other gases and collected for the graphitisation step. At the same time, the C/N atomic ratio can be measured: as described in paragraph 5.2.1. This value can represent a useful indication to evaluate the possible presence of contaminants in the sample. The "good" range is considered to be between 2.9 and 3.6.

As usual in LABEC sample preparation procedure, when it is possible, two pellets were prepared for each sample to be measured.

Table 5.3 - Measured C/N ratios in ulna and humerus samples. C/N ratio in case of Fi3064 is not reported because the acquired chromatogram was too noisy to be accurately fitted.

SAMPLES	LAB CODE	C/N (± 0.2)
ULNA_ref	Fi2840	3.5
	Fi2844	3.6
ULNA_PARA_LON	Fi2841	5.4
	Fi2843	3.6
ULNA_PARA_Chl_LON	Fi3064	-
	Fi3067	3.2
HUMERUS_ref	Fi2853	3.6
	Fi2856	3.5
HUMERUS_PARA_LON	Fi2855	3.6
HUMERUS_PARA_Chl_LON	Fi3066	3.3
	Fi3069	3.1

Analysing the data shown in table 5.3, all samples, except Fi2841, present C/N ratios that are slightly less than or equal to the acceptable upper limit for a good preserved collagen. Indeed, only Fi2841 is characterized by a C/N ratio well besides the limit, thus indicating a high probability to be strongly contaminated or largely degraded.

The case of ULNA_PARA_LON sample, in which two collagen fragments of the same sample are characterised by two very different C/N ratios, suggests that the possible contaminations are not homogeneously distributed in the whole sample.

5.4.2 AMS measurements

Table 5.4 shows the AMS measurements results. When the two measured fractions of each of the bone samples (see the lab. codes in table 5.3) were consistent between each other, their weighted average was calculated as the best estimate of radiocarbon concentration. When this is not the case, results obtained for each of the two measured pellets are separately shown.

Table 5.4 - Measured ^{14}C concentrations and corresponding radiocarbon ages.

SAMPLES	^{14}R (pMC)	t_{RC} (yr BP)
ULNA_ref	87.60 ± 0.45	1065 ± 40
ULNA_PARA_LON (Fi2841)	56.55 ± 0.44	4580 ± 60
ULNA_PARA_LON (Fi2843)	83.2 ± 1.7	1470 ± 160
ULNA_PARA_Chl_LON_1	85.47 ± 0.36	1075 ± 50
ULNA_PARA_Chl_LON_2	87.57 ± 0.28	1066 ± 25
HUMERUS_ref	88.25 ± 0.40	1005 ± 50
HUMERUS_PARA_LON	82.95 ± 0.54	1500 ± 50
HUMERUS_PARA_Chl_LON_1	87.89 ± 0.51	1040 ± 45
HUMERUS_PARA_Chl_LON_2 (Fi3321)	87.33 ± 0.36	1088 ± 35
HUMERUS_PARA_Chl_LON_2 (Fi3323)	85.65 ± 0.33	1244 ± 30

As expected, in both cases of ulna and humerus, the fractions prepared just following the "normal" extraction procedure are clearly contaminated (see ULNA_PARA_LON and Humerus_PARA_LON).

Moreover, in the case of ULNA_PARA_LON, we have measured a great difference between the two pellets Fi2841 and Fi2843. This result suggests that the contaminations are not homogeneously distributed in the material. Pre-treating the contaminated samples (ULNA_PARA_Chl_LON) according to the chloroform-based procedure, the measured concentrations are consistent with the expected value. In both cases four extractions were performed.

The HUMERUS_PARA_Chl_LON shows a slightly different behaviour with respect to that described for ULNA_PARA_Chl_LON samples. In fact, in the case of HUMERUS_PARA_Chl_LON_1, four extractions in chloroform were sufficient to remove the contamination. On the contrary, in the case of HUMERUS_PARA_Chl_LON_2, the radiocarbon concentrations are not consistent in the two measured pellets processed from the same sample. In particular, the sample Fi3321 is consistent with the expected value, while in the sample Fi3323 the contamination seems not to be completely removed. Probably, at least another

extraction in chloroform would have been necessary for the HUMERUS_PARA_Chl_LON_2 sample.

5.4.3 FT-IR analyses

Following the same approach used in the case of the wood test samples discussed in paragraph 4.2.4, we first performed FT-IR analyses on the solid samples before combustion, to check the possible presence of the Paraloid marker. We decided to measure the extracted collagen and not the raw bone powder, because in the latter case we may have expected interferences in the spectra due to the complex bone matrix. Anyway, an interference due to the bands of collagen, in particular with amide I (1650 cm^{-1}), can be also expected. In addition, we performed FT-IR measurements on the liquid extracts collected during the chloroform-based treatment, to verify the removal of the resin.

Figure 5.3 shows the FT-IR spectra acquired on the collagen extracted from the ulna reference sample and one of the contaminated samples before radiocarbon dating.

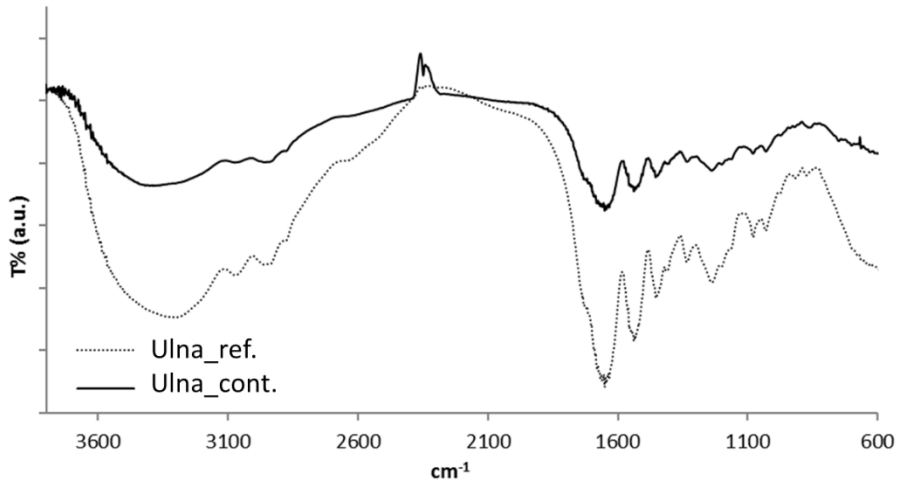

Figure 5.3 – FT-IR spectra collected on collagen samples. Ulna_ref. is acquired on collagen extracted from the ulna reference sample, while Ulna_cont. is acquired on collagen extracted from one of the ulna contaminated samples. In both spectra, the bands due to amides (1650 $cm^{-1,}$ 1550 $cm^{-1,}$ 1450 cm-1) are well visible.

In both spectra, the absorption bands due to amides, the main protein components of collagen, are well visible. These bands are about 1650 cm^{-1} (Amide I), 1550 cm^{-1} (Amide II) and 1450 cm^{-1} (Amide III), and they form a sort of scale model quite easy to recognise, especially in sufficiently well preserved bones. In addition, the presence of the amides can be also confirmed by the N-H stretching broad band about 3355cm^{-1}. The spectrum acquired on the contaminated collagen does not give any information about the contamination due to Paraloid B72. A weak knee at about 1740cm^{-1} is present on both spectra. Actually, the functional group C=O is also present in the amide structure. A possible explanation can be due considering an interference between the broad absorption band of Amide I and the characteristic Paraloid band or the fact that the analysed collagen fragment is not contaminated. In fact, as we have observed during the AMS and the C/N measurements, the contaminants cannot be homogeneously distributed.

As described in the case of the contaminated wooden samples, the solutions collected during the extraction with chloroform could contain Paraloid B72, but in a very diluted state. To permit the FT-IR analyses, for each treated sample, the four solutions were dried in a rotary evaporator, to remove the chloroform itself, and eventually the residues were deposited on KBr plates. This process was repeated for both bone samples (Ulna and Humerus).

Figure 5.4 shows the spectra acquired on extracts collected processing ULNA_PARA_Chl_LON bone sample. None of the spectra, not even in the liquid collected after the first extraction, presents the characteristic band about 1740 cm^{-1}. The absence of this absorption band may be explained considering that, despite the sample was collected near consolidated and so possibly contaminated area, any traces of Paraloid B72 were not in the collected material.

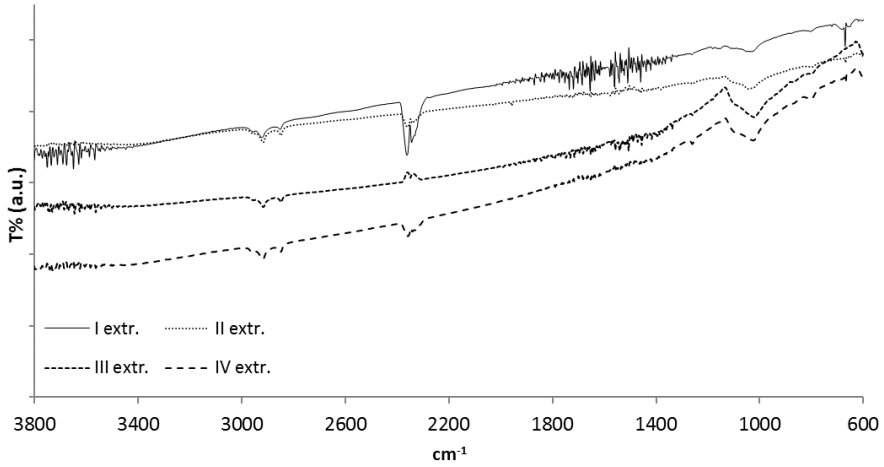

Figure 5.4 – FT-IR spectra acquired on liquid extracts during the chloroform-based treatment. The band about 1740 $cm^{-1}$is not visible even in the first bath.

Figure 5.5 shows the FT-IR spectra collected on liquid extracts while processing HUMERUS_PARA_Chl_LON_2 sample. Observing the figure, it is evident the presence of the band about 1740 cm^{-1} that characterises the presence of Paraloid B72. The intense band is visible in all the spectra. In this case, performing four extractions was not probably sufficient to completely remove the contaminant from the material. A further extraction would have been necessary to verify whether the removal could be complete. The comparison of these data with the radiocarbon results is very interesting. Indeed, the radiocarbon concentrations measured on the two pellets prepared from this HUMERUS_PARA_Chl_LON_2 sample gave us contradictory results: Fi3321 is compatible with HUMERUS_ref, while Fi3323 is not consistent with the expected value, thus confirming what can be inferred from the FT-IR analyses.

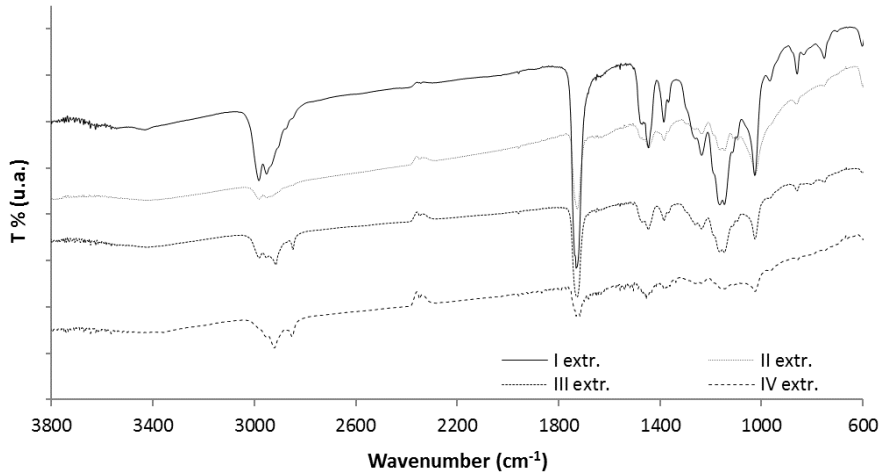

Figure 5.5 - FT-IR spectra acquired on liquid extracts during the chloroform-based treatment. The bands about 1740 cm^{-1}due to presence of contaminant is well visible also in the 4th extract.

The monitoring of the effectiveness of the removal procedure was usefully performed by the applying of the FT-IR technique. This approach could become methodological during the samples preparation.

5.5 Bones from Bronze Age Cyprus

During the three years of PhD course, I took part to a dating campaign on samples collected during several archaeological surveys in the area of Erimi-Laonin tou Porakou, in the south of Cyprus. Erimi-Laonin tou Porakou was first identified in 2007. Since then, the archaeological area has been systematically excavated as a joint project of the Universities of Turin and Florence, in collaboration with the Department of Antiquities of Cyprus [Bom2011]. The site is very interesting for the archaeologists because it shows an ancient occupation sequence and several functional areas. In fact, it presents an organisation of distinct working and storing spaces. In particular, in the investigated area, the archaeologists have identified a workshop complex, a domestic quarter and two areas dedicated to burials (Vounaros and Southern cemeteries). At the present state of research, on the basis of the

interpretation of the stratigraphic deposit and analysis of the ceramic assemblage, two main periods of occupation are proposed: first during the Bronze Age and later during the Late Hellenistic and Roman Age.

Figure 5.6 shows the area interested by the archaeological investigation. The collected samples are many and of various materials, for example metal slags, pottery, charcoals and bones.

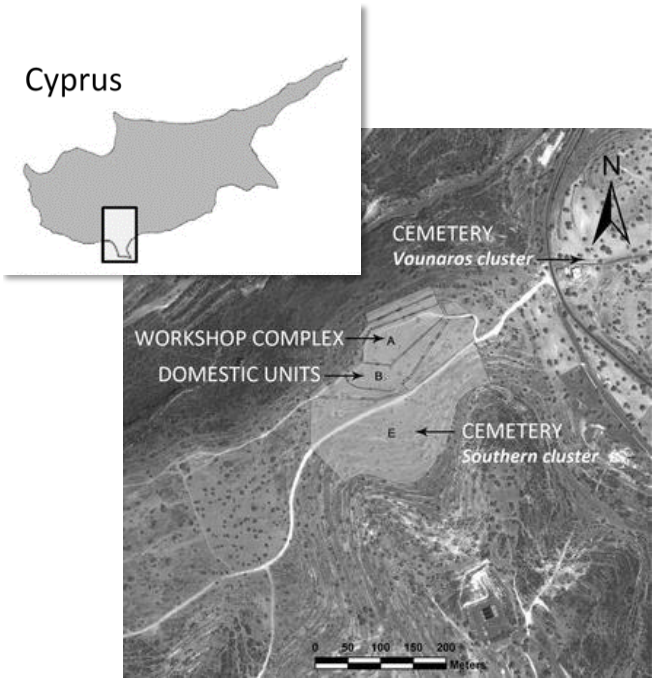

Figure 5.6 – The site of Erimi-Laonin tou Porakou in the southern Cyprus.

At LABEC laboratory, we radiocarbon dated charcoals and bones.

Among all the collected bone samples, three of them had been consolidated using a glue based on polyvinyl acetate, commercially sold as Vinavil ® K60. This glue is used especially for the consolidation of archaeological finds and ceramics.

As an example, Figure 5.7 shows the image on one of the consolidated sample (T.228 B37) taken by optical microscope. In the figure, the red arrow shows the translucent material applied to mineral matrix.

Figure 5.7 – The red arrow highlights the consolidant applied to the bone sample.

We thus decided to apply the chloroform-based pre-treatment, already shown to be effective to remove Paraloid B72 on wood and bones, to these samples too.

Processing these bone samples from Cyprus, the possibility to recover good quality collagen is very low. In particular, the bones collected in this area are suffering of great diagenesis. In fact, the environmental conditions do not favour the collagen preservation. This area is characterised by a calcareous soil, with an alkaline pH. In addition, this region presents hot temperature especially during summer, when 40°C are reached. Both these factors contribute to deteriorate the collagen.

During the pre-treatment, a special attention was dedicated to the demineralisation phase.

5.5.1 Radiocarbon measurements on consolidated bones

As it is possible to observe in figure 5.8, the size of these bones was not enough to allow us to separately collect two fragments, one to be used as reference and one to be treated in chloroform.

Figure 5.8 – T.228 B37 bone sample. Its size cannot permit to collect two different fragments.

Therefore, the chloroform-based procedure was applied to each sample as a whole, after the usual mechanical cleaning and grinding process. Also in these cases, we performed four extractions. Afterwards, the typical collagen extraction procedure was applied.

Unfortunaly, only in one case, the recovered collagen was sufficient for the radiocarbon concentration measurement.

The measured radiocarbon data about T.228 B37 are summarised in table 5.5.

Table 5.5 – Measured radiocarbon concentration and corresponding radiocarbon age in the two pellet of T.228 B37 sample.

SAMPLES	^{14}R (pMC)	t_{RC} (years BP)
Fi3165	65.63 ± 0.30	3385 ± 40
Fi3167	65.67 ± 0.32	3390 ± 40
T.228 B37	65.60 ± 0.22	3390 ± 30

To verify if this result can be considered consistent within the archaeological framework of origin, we can compare it to the other uncontaminated bone samples that were radiocarbon dated. In table 5.6 the radiocarbon measured concentration of

uncontaminated bone samples and the radiocarbon measured concentration of the contaminated bone sample pre-treated using the chloroform-based process are shown.

Table5.6 – Radiocarbon measured concentration and corresponding radiocarbon age of bone samples collected during the archaeological campaign. T.228 B37 is processed adding the step of chloroform, while the other samples are processed according to the modified Longin method.

SAMPLE	$[^{14}R]$ (pMC)	t_{RC} (yr BP)
T228 B37	65.60 ± 0.22	3390 ± 30
T 238 B2	65.98 ± 0.82	3340 ± 60
T 230_1	64.92 ± 0.32	3470 ± 40
T 230_2	66.81 ± 0.33	3240 ± 40
T 248_1	63.72 ± 0.32	3620 ± 40
T 248_2	64.12 ± 0.44	3570 ± 55
T 248 _3	64.92 ± 0.57	3470 ± 70
T 428_1	62.86 ± 0.39	3730 ± 50
T 428_2	64.36 ± 0.36	3540 ± 45

The radiocarbon concentration measured in T.228 B37 is consistent with the radiocarbon measured concentration of the uncontaminated sample collected in Erimi-Laonin tou Porakou archaeological site. The radiocarbon dated bones have been analysed as a single phase, showing the use of the necropolis in a range of reasonable time from the archaeological point of view. Figure 5.9 shows the calibrated data for all the samples reported in table 5.6. The calibrated data, obtained using the Ox.Cal 4.2, are represented in grey. Considering the historical period of settlement in this area, the contaminated bone treated according to chloroform-based procedure is well connected in the archaeological framework, thus we can suppose that the removal of consolidant was effective, in this case too. This result suggests us the possibility to use the chloroform-based procedure also in the case of contamination different of Paraloid B72.

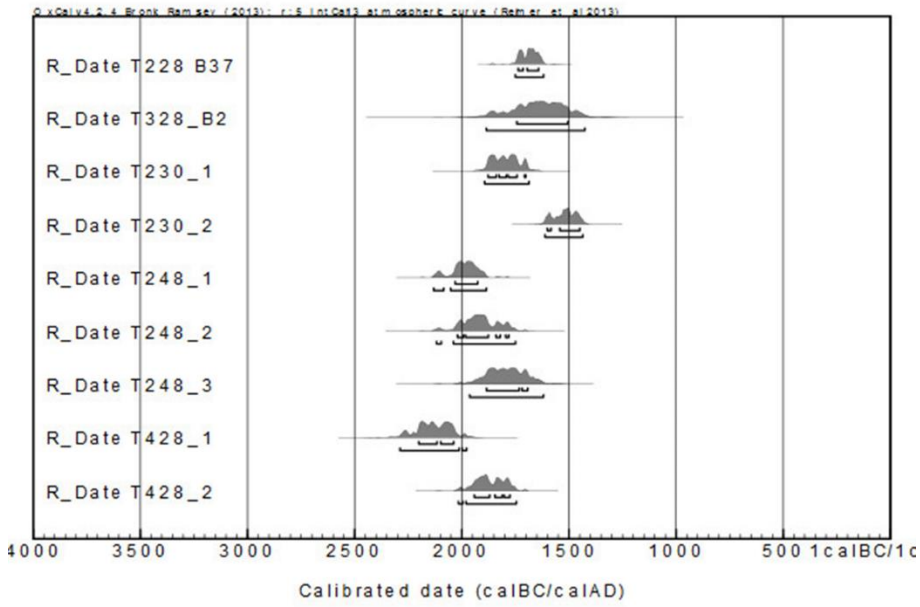

Figure 5.9 – Sequence of calibrated ages of bone samples collected in Erimi-Laonin tou Porakou. The data were calibrated using OxCal 4.2.

Conclusions

In this thesis, I have discussed the case of possible contaminations - and their removal - introduced by synthetic resins on restored sample that are radiocarbon dated by Accelerator Mass Spectrometry (AMS). Among the products used for restoration and consolidation purpose in the field of Cultural Heritage, we focused on Paraloid B72. In particular, a simple pre-treatment procedure has been proposed and the feasibility to use the Fourier Transform Infrared technique (FT-IR) as a supporting tool during the sample preparation has been investigated. FT-IR technique is chosen for its high capability to discriminate organic compounds and for the small amount of required material to acquire a spectrum. This is a very important feature, dealing with samples collected in the field of Cultural Heritage.

During the first part of my PhD course, the effectiveness of the chloroform-based pre-treatment procedure has been characterised both on historical restored wooden samples and on test wooden samples of known radiocarbon concentration, that had been contaminated on purpose.

We investigated the relationship between the number of extractions, performing up to four extraction, and the procedure efficacy both by AMS and FT-IR.

The complex matrix in the sample, derived from the presence of contaminant mixed to untreated material, does not permit to discriminate the presence of the contaminant itself. In fact, the absorption band at 1740 cm^{-1} due to the stretching bond of C=O, chosen as Paraloid B72 marker, is present also in raw wood. Anyway, for

each test sample, FT-IR spectrum was acquired to check the behaviour of the peak about 1740 cm^{-1}, observing that the band increase as the contamination volume increase.

The problem of interfering bands, added to the great difficulty to prepare homogenous KBr pellets, has led to use of FT-IR to analyse the liquid extracts collected after each of the extractions, performed during the chloroform-based procedure.

We noticed an intense peak around 1740 cm^{-1} in the FTIR spectra acquired for the first and the second extraction, while in the third and the fourth spectra, the band cannot be discriminated with respect to the background noise. As far as AMS analyses are concerned, we observed that the measured ^{14}C concentrations were basically consistent with the expected value already after the second extraction (within the experimental uncertainties).

Moreover, we verified that the removing of Paraloid B72 does not depend on the contaminat volume applied on the sample, but we can guess that the most important factor may be the Paraloid state of preservation.

In addition, the chloroform-based procedure was tested on different consolidated material: bones.

Following the same approach used in the case of the wooden test samples, FT-IR spectra were acquired on collagen, the suitable fraction for radiocarbon dating. FT-IR spectra on the raw collagen just give us a very poor information, first because the possible interference of the strong Amide I (1650 cm^{-1}) band with the Paraloid marker at 1740 cm^{-1}. In addition, we noticed that difficulties can also arise from the non-homogeneity of the distribution of contaminant in the sample, being the AMS measurements performed on a different sample from the sample that is analysed using FT-IR technique. This point can be overcome using Attenuated Total Reflectance (ATR), since this technique does not require any specific sample preparation. Thus, the same sample can be used first to acquire ATR spectrum and then for AMS measurements.

As in the case of wooden sample, the most useful information we can get through FT-IR analyses is those collected on the liquid extracts, that were obtained after each of the extractions during chloroform-based procedure. When in the FT-IR spectra the marker band is not visible, we can be reasonably sure that Paraloid is removed. The confirm of these results can be achieved by the comparison with the AMS measurements. The analyses on bone samples has however suggested another important observation: performing up to four extractions may not be sufficient to completely remove the contaminant from the material (see the case of the analysed humerus). Definitely, FT-IR spectra acquired on extracts during the sample preparation step can be a great helpful tool to verify whether the sample pre-treatment has been successful or not. This allow us to decide how many extractions are required during the process.

Considering the powerful aspects of spectroscopic techniques, the use of IR spectroscopy should be regularly introduced to monitor sample preparation for those restored sample to be radiocarbon dated.

Appendix A

Fourier Transform Infrared Spectroscopy (FT-IR) is one of the tecniques that can be employed when measuring IR absorption. Since the 1950s, FT-IR has shown helpful as a key analytical method in laboratory. This tecnique is also very common in the field of art conservation and restoration, in order to study the functional groups that characterise a material, both organic and inorganic compounds [Der1999]. One of advantages of this tecnique is that it requires a small amount of sample to acquire a spetrum. This is definitely one of the strengths when dealing samples in the Cultural Heritage field.

Infrared spectroscopy

With the term Infrared spectroscopy we typically consider the interaction of the electromagnetic radiation with matter at the infrared wavelenghts.

Electromagnetic radiation is characterised by spectral regions that depend on energy (or wavelenght), as it shown in Figure A.1. In the figure, a zoom on the Mid-IR region, that covers the frequency ranges between 4000 and 500 cm^{-1} and that correspond to the most used interval in diagnostics, is represented.

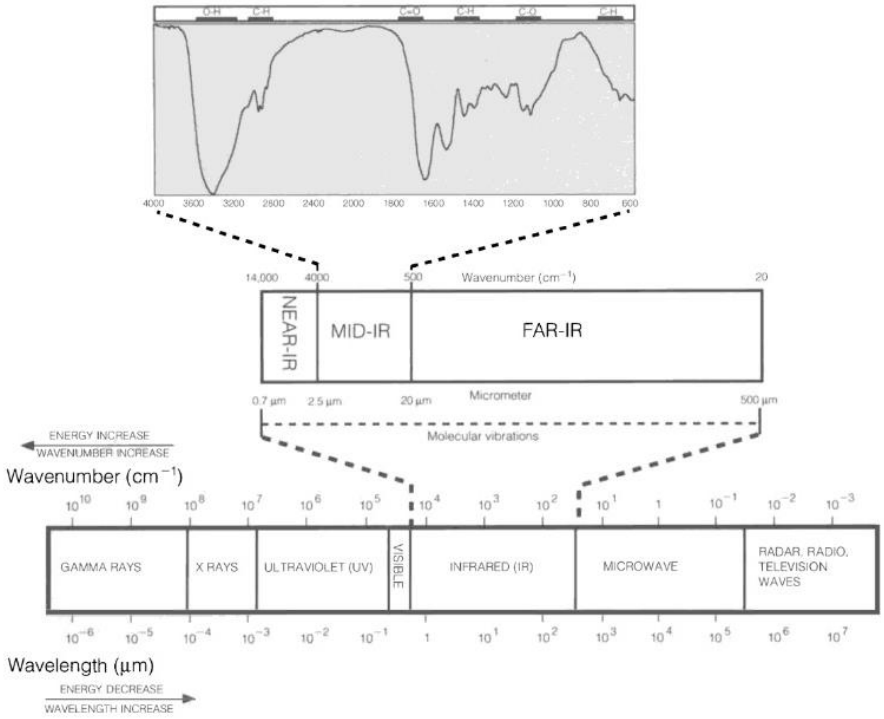

Figure A.1 - Different spectral regions of electromagnetic radiation. The Infrared region is highlighted [Der1999].

Based on the work developed by Bohr, who described the absorption theory for atoms at the beginning of the 20th century, few years later some scientists expanded this theory to molecules. The Infrared radiation is too low energetic to acts on the electron state within an atom, but it can be absorbed by molecular bonds. The IR energy is converted to translational, rotational and vibrational transitions that correspond to molecular movements, becoming a useful tool to identify and characterise the structure of the molecules themselves. Not all the molecules respond to IR radiation. The "selection rule" is linked to the changing of the electric dipole moment. The change in the dipole moment creates an electric field that needs a discrete and specific unit of energy so that that transition exists. If there are no changes in the dipole moment, the molecule is not sensitive to the adsorption in the IR range.

An active IR molecule with N atoms can have 3N degrees of freedom. Movements can be translational, rotational and vibrational. For example, if we consider a diatomic molecule, we observe three degrees of translational freedom, two degrees of rotational freedom and only one of vibrational freedom [Stu2004]. The latter corresponds to the stretching and the compression of the bond between the two atoms. In general, the number of the degrees of vibrational freedom are 3N-5 in case of linear molecules, or 3N-6 in case of non-linear ones. For these polyatomic molecules, vibration modes can be due to changes not only in the bond length (stretching) but also in the bond angle (bending). Figure A.2 shows an example of stretching and bending movements.

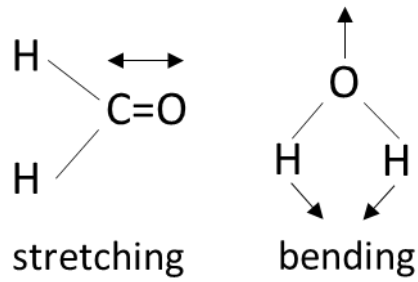

Figure A.2 - Stretching and bending vibration modes. In the stretching vibrations, there is a change in length bond, in the bending vibration, the change involves the bond angle.

The molecule adsorbs the Infrared radiation only at the frequency of the one of the fundamental modes of vibrations, so that only the interested functional groups is interested by vibration, while the rest of molecule is left unchanged.

The spectrum

An IR spectrum is a crucial tool to allows identifying the organic and inorganic materials because the absorption bands are attributable to specific movements of bonds. In particular, the so-called functional groups are specific bonds that are responsible for the characteristic chemical reactivity of the molecules.

The IR spectrum shows a sequence of absorption bands recorded as a function of the wavenumber (or wavelength). The absorption bands are characterised by three important parameters such as frequency, shape and intensity [Der1999]. Band frequency is related to the presence of certain functional groups in the analysed material, while its shape can give information on the purity of the material itself. Indeed, a not completely symmetrical shape can indicate the presence of overlapping bands. Finally, the band intensity, as relative to the other bands present in the spectrum, gives information on the amount of a functional group present in that specific sample. Obviously, the presence of a functional group in a spectrum does not mean an univocal identification of the material; on the contrary the absence of a functional group can be used to eliminate a "suspect" compound.

When a spectrum is acquired on a sample collected from a composite material, the spectrum interpretation can appear very complex. In the field of Cultural Heritage, a typical example of a composite material is a sample collected from an artwork, since a great variety of natural and synthetic materials are employed together by the artists. Furthermore, there can be all the materials added in restoration over the centuries.

An IR spectrum can be divided into different spectral regions corresponding to different movement modes of the functional groups. The principal ranges are:

- H-X stretching region (4000-2500 cm^{-1}), where X indicates any element that can create a stretching bond with hydrogen;
- Triple bond region (2500-2000 cm^{-1});
- Double bond region (2000-1500 cm^{-1});
- Fingerprint region (1500-600 cm^{-1}).

In the first region, the fundamental vibrations are due to O-H, C-H and N-H stretching. In the triple bond stretching region, functional groups as C≡C and C≡N occur, while in the double bond region, the principal bands are due to C=C and C=O stretching. The fingerprint region is peculiar for each molecule, because it is a combination of overlapping bands of varying intensity. Its specificity can confirm an assignment to compound by direct comparison to reference spectrum.

Basically, the most efficient instruments to obtain absorption spectra in the mid IR are based on the possibility to collect at the same time all frequencies of the IR spectrum. For this purpose, a Michelson interferometer is used to acquire the combination of the IR radiation emitted by a polychromatic source and the radiation absorbed by the abalysed sample in an interferogram (see figure A.3).

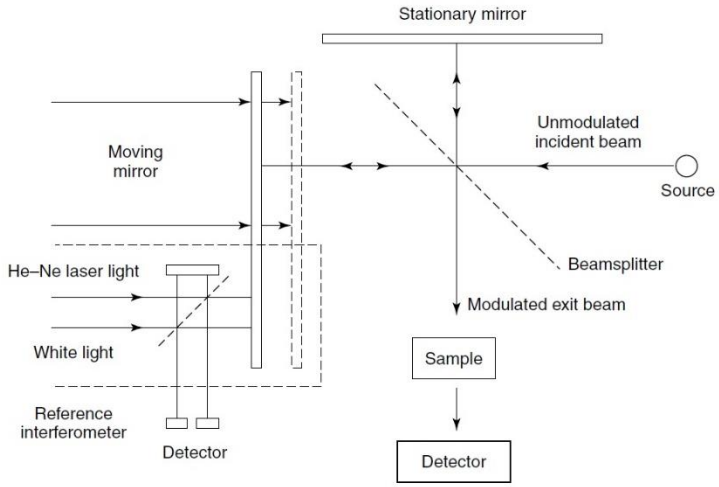

Figure A.3 - Schematic of a Michelson interferometer in a FT-IR spectrometer (reproduced from Stu2004).

The Michelson interferometer consists of two perpendiculary plane mirrors, one of which can move in a perpendicular direction in front of the radiation source, while the other is stationary (see Figure A.3). A semi-reflecting beamsplitter, a film chosen according to the IR region to be examinated, is positioned in the middle of the IR path. Ideally, if a IR beam passes through a beamsplitter, 50% of the incident radiation will be reflected to the stationary mirror, while the other 50% will be transmitted to the moving mirror, returning to the beamsplitter where they ricombine and interfere. Scanning the moving mirror produces differences in the optical path of the IR radiation contributing to the creation of an interference pattern (see Figure A.4), acquired by an IR-sensitive detector, after passing through the sample itself. In the mid-IR region, the detector is a pyroelectric device incorporating deuterium tryglycine sulfate (DTGS) in a temperature-resistant alkali halide window.

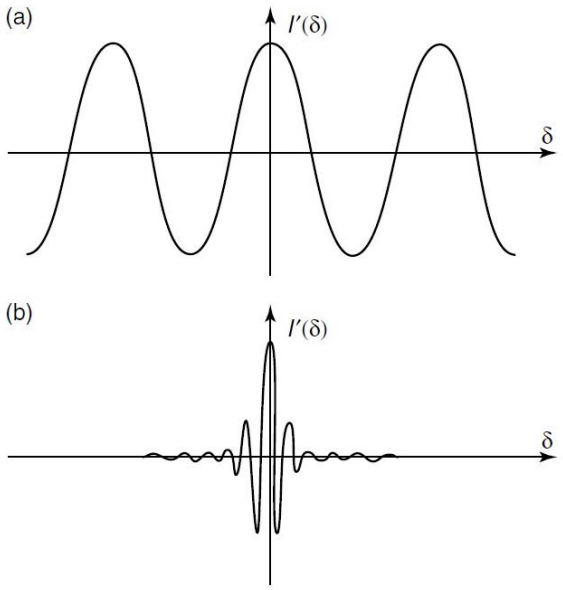

Figure A.4 - Interferograms obtained in case of monochromatic source (a) and in case of polychromatic source (b). The second one is more complicated because all of the spectral information are simultaneously collected [Stu2004].

In this way, we obtain an interferogram in the time domain, but these data are quite difficult to process. The mathematical tool that allows passing from the time domain to the frequency domain, which is typically easier to handle, is indeed the Fourier Transform. Finally, a FT-IR spectrum is usually plotted in trasmittance pergentage (%T) versus IR frequency (wavenumbers; cm^{-1}).

The transmission method permits the analysis on gas, solid and liquid samples. It is a minimally invasive technique, since, generally, few milligrams are needed (1-5 mg).

In order to perform a transmission analysis, the sample is placed in a supporting material. Ideally, this material should be IR transparent to the incident radiation, i.e. it would not adsorb any of the IR radiation. One of the most used materials is Potassium Bromide (KBr): this compound is very useful in the mid-IR region, but unfortunately, it is water sensitive, so it can be used for most of the analysed materials other than aqueous solutions.

In the case of solid samples the material is ground, using an agate mortar and pestle, mixing with KBr powder in order to constituite a thin transaparent pellet after a pressure of about $1.5x10^5$ kg/m^2. Another procedure is to deposit few drops of solution containing the sample on a KBr plate and then the FT-IR spectrum is acquired after solvent evaporation.

The instrument used during this PhD work is Shimadzu FTIR-8400S spectrometer with a resolution of 2.0cm^{-1} and 16 scans per sample.

References

[Bag2014] Baglioni P., Bert D., Bonini M., Carretti E., Dei L., Fratini E., Giorgi R., *Micelle, microemulsions and gels for the conservation of Cultural Heritage*, Advanced in Colloid and Interface Science, Vol 205, p. 361-371

[Bag2009] Baglioni P., Giorgi R., Dei L., *Soft condensed matter for the conservation of Cultural Heritage*, Comptes Rendus Chimie, Vol. 12, p. 61-69

[Bom2011] Bombardieri L., *Memory and change, sharing and competition. The appointment of spaces in settlements and necropoles within the Bronze Age cypriot communities*, Munari editore (2011)

[Bor1995] L.Borgioli et al, *Removal of hydrophobic impurities from pictorial surfaces by means of heterogeneous system*, Science and Technology for Cultural Heritage 4, p.67-74

[Bow1990] Bowman S., *Radiocarbon dating*, British Museum Publication Ltd (1990)

[Bru2001] F. Bruhn et al., *Chemical removal of conservation substances by Soxhlet type extraction*, Radiocarbon 43 (2A), p. 229-237

[Bur2013] Burr G.S., *Causes of temporal ^{14}C Variation*, Encyclopedia of Quaternary Science, in S.A. Elias (E.D.), Elsevier B.V., II edition (2013)

[Caf2013] Caforio L., Fedi ME., Liccioli L., Salvini A., *The issue of contamination by synthetic resins in radiocarbon dating: the case of a painting by Ambrogio Lorenzetti*, Procedia Chemistry, Vol.8. p. 28-34

[Cal2011] Calzolai G., Bernardoni V., Chiari M., Fedi ME., Lucarelli F., Nava S., Riccobono F., Taccetti F., Valli G., Vecchi R., *The new sample preparation line for*

radiocarbon measurements on atmospheric aerosol at LABEC, Nucl. Instr. and Meth. B 269, p. 203-208.

[Car2003] E.Carretti e L.Dei, *Physicochemical characterization of acrylic polymeric resins coating porous materials of artistic interest,* Progress in organic coatings 49,p.282-289

[Car2008] E.Carretti et al. (2008), *A new class of gels for the conservation of painted surfaces,* Journal of Cultural Heritage 9, p.386-393

[Cap2012] Capano M., Marzaioli F., Passariello I., Pignatelli O., Martinelli N., Gigli S., Gennarelli I., De Cesare N., Terrasi F., *Preliminary radiocarbon analyses of contemporaneous and archaeological wood from the Ansanto valley (Southern Italy).* Radiocarbon Vol. 54, p. 701-714.

[Chi2001] Chiantore O., Lazzari M., *Photo-oxidative stability of Paraloid acrylic protective polymers,* Polymer 42, p. 17-27

[Cia2009] Ciancio Rossetto P., *Portico d'Ottavia, un monumento esemplare per il recupero e il reimpiego*, École française de Rome, Sapienza Università di Roma, Dipartimento di Storia dell'Architettura, Restauro e Conservazione dei Beni Architettonici, p.255-262

[Col2009] Colombini M., Modugno F., *Organic Mass Spectrometry in Art and Archaeology,* John Wiley & Sons, Ltd (2009)

[Col2000] Colombini M., Modugno F., Giannarelli S., Fuoco R., Matteini M., *GC-MS characterisation of paint varnishes,* Microchemical Journal Vol 67, p. 385-396

[Cop1994] Coplen T.B., *Reporting of stable Hydrogen, Carbon, and Oxygen isotopic abundances,* Pure & Appl. Chem., Vol. 66, No. 2, p. 273-276

[Cra1954] Craig H., *Carbon 13 in Plants and the Relationships between Carbon 13 and Carbon 14 Variations in Nature,* The Journal of Geology, Vol. 62, No. 2, p. 115-149

[Del2007] D'Elia M., Gianfrante G., Quarta G., Giotta L., Giancane G., Calcagnile L., *Evaluation of possibile contamination sources in the ^{14}C analysis of bone samples by FTIR spetroscopy*, Radiocarbon, Vol. 49, No. 3, p. 201-210

[DeN1985] De Niro M.J., *Postmortem preservation and alteration of in vivo bone collagen isotope ratios in relation to palaeodietary reconstruction,* Nature 317, p. 806-809

[Der1999] Derrik M., Stulik D., Landry J.M., *Scientific tools for conservation Infrared Spectroscopy in Conservation*, The Getty Conservation Institute Los Angeles (1999)

[Fed2015] Fedi ME., Liccioli L., Castelli L., Czelusniak C., Giuntini L., Mandò PA., Palla L., Taccetti F., *Memory effects using an elemental analyser to combust radiocarbon samples: failure and recovery*, Nuclear Instrument and Method in Physics Research B 361, p. 376-380

[Fed2014] Fedi ME., Caforio L., Liccioli L., Mandò PA., Salvini A., Taccetti F., *A simple and effective removal procedure of synthetic resins to obtain accurate radiocarbon dates of restored artworks*, Radiocarbon, Vol. 56, No. 3, p. 969–979

[Fed2007] Fedi ME., Cartocci A., Manetti M., Taccetti F., Mandò PA., *The ^{14}C AMS facility at LABEC, Florence*, Nuclear Instrument and Method in Physics Research B 259, p. 18-22

[Fel1994] Feller R.L., *Accelerated Aging, photochemical and thermal aspects*, The Getty Conservation Institute Los Angeles (1994)

[Fri1999] Fringeli U.P., *ATR and Reflectance IR Spectroscopy*, Applications, Encyclopedia of Spectroscopy and Spectrometry (Second Edition), Academic Press, p. 94-109

[Kli1999] van Klinke G.J., *Bone Collagen Quality Indicators for Palaeodietary and Radiocarbon Measurements*, Journal of Archaeological Science 26, p. 687-695

[Koo1986] Koob S.P., *The use of Paraloid B-72 as an adhesive: its application for archaeological ceramics and other materials,* Studies in Conservation 31, p. 7-14

[Kut2013] Kutschera W., *Applications of accelerator mass spectrometry*, International Journal of Mass Spectrometry, p. 203-218

[Hau1972] Haut R.C., Little R.W., *A constitutive equation for collagen fibers*, Journal of Biomechanics, Vol. 5, p. 423-430

[Hor2010] Horie V., *Materials for conservation. Organic consolidants, adhesives and coatings*, Routledge, London and New York (2010)

[Hua2013] Hua Q., Barbetti M., Rakowski A.Z., *Atmospheric radiocarbon for the period 1950-2010*, Radiocarbon, Vol. 55, No. 4, p. 2059-2072

[Hua2009] Hua Q., *Radiocarbon: a chronological tool for the recent past*, Quaternary Geochronology 4, p. 378-390

[Hua2004] Hua Q. and Barbetti M., *Review of tropospheric bomb ^{14}C data for carbon cycle modeling and age calibration purpose*, Radiocarbon 46, p. 1273-1298

[Le1998] Le M.C., van der Plicht J., Groening M., *New ^{14}C reference materials with activities of 15 and 50 pMC*, Radiocarbon, Vol. 40, No. 1, p. 11-20

[Lev1989] Levin I., Schuchard J., Kromer B., Muennich K.O., *The continental european Suess Effect*, Radiocarbon Vol. 31, p. 431-440

[Lic2012] Liccioli L., *Datazione con radiocarbonio di opere d'arte restaurate: effetti di contaminazione da resine sintetiche e loro rimozione*, Tesi di laurea magistrale, Università degli Studi di Firenze A.A. 2010/2011

[Lin1992] Lin S.Y., Dence C.W., *Methods in Lignin Chemistry*, Springer (1992)

[Lin2013] Lindauer S., Kromer B., *Carbonate sample prepatation for ^{14}C dating using an elemental analyser*, Radiocarbon Vol.55, p. 364-372

[Lon1971] Longin R., *New method of collagen extraction for radiocarbon dating*, Nature 230, p. 241-242

[Man1983] Mann W.B., *An international reference material for radiocarbon dating*, Radiocarbon Vol. 25, No. 25, p. 519-527

[McD1978] Mc Donald R., *Infrared spectrometry*, Analytical Chemysty, p. 282-299

[Min2010] Minami M., Goto A.S., Omori T., Ohta T., Nakamura T., *Comparison of $\delta^{13}C$ and ^{14}C activities of CO_2 samples combusted in closed-tube and elemental-analyzer systems*, Nuclear Instruments and Methods in Physics Research B 268, p. 914-918

[Pal2015] Palla L., Castelli L., Czelusniak C., Fedi ME., Giuntini L., Liccioli L., Mandò PA., Martini M., Mazzinghi A., Ruberto C., Schiavulli L., Sibilia E., Taccetti F., *Preliminary measurements on the new TOF system installed at the AMS beamline of INFN-LABEC*, Nuclear Instrument and Method in Physics Research B 361, p. 222-228

[Ras2009] Rasmussen K.L., van der Plicht J., Doudna G., Nielsen F., Hojrup P., Stenby E. H., Pedersen C., *The effects of possible contamination on the radiocarbon*

dating oh the Dead Sea scrolls II: empirical methods to remove castor oil and suggestion for redating, Radiocarbon, Vol 51, p 1005-1022

[Rei2002] Reiche I., Vignaud C., Menu M., *The cristallinity of ancient bone and dentine: new insights by transmission electron microscopy*, Archaeometry, Vol. 44, p. 447-459

[Rei2013] Reimer P.J. et al, *IntCal13 and Marine13 radiocarbon age calibration curves 0–50,000 years cal BP*, Radiocarbon, Vol. 55, No. 4, p. 1869–1887

[Rei2009] Reimer P.J. et al, *IntCal09 and Marine09 radiocarbon age calibration curves, 0–50,000 years cal BP*, Radiocarbon, Vol. 51, No. 4, p. 1111–1150

[Sci2013] Scirè Calabrisotto C., Fedi ME., Caforio L., Bombardieri L., Mandò PA., *Collagen quality indicators for radiocarbon dating of bones: new data on Bronze Age Cyprus*, Radiocarbon, Vol. 55, No. 2–3, 2013, p. 472–480

[Sch2007] Scharf A., Luppold T. Rottenbach A., Kritzler K., Ohneiser A., Kretschmer W., *Status report on the Erlangen AMS facility*, Nuclear Instruments and Methods in Physics Research B 259, p. 50-56

[Sou2010] Southon J.R., Magana A.L., *A comparison of cellulose extraction and ABA pretreatment methods for AMS ^{14}C dating of ancient wood*, Radiocarbon, Vol. 52, No. 2-3, p. 1371-1379

[Ste2011] Sternström K.E., Skog G., Georgiadou E., Genberg J., Johansson A., *A guide to radiocarbon units and calculations*, Internal report Lund University LUNFD6 (NFFR-3111), p. 1-17

[Stu2004] Stuart B., *Infrared Spectroscopy: foundamentals and applications*, WILEY (2004)

[Sue1955] Suess H.E., *Radiocarbon Concentration in Modern Wood*, Science, Vol. 122, p. 415-417

[Tam2014] Tamburini D., Luceiko J.J., Modugno F., ColombiniM., Pallecchi P., Giachi G., *Microscopic techniques (LM,SEM) and multi-approach (EDX,FT-IR, GC/MS, Py-GC/MS) to characterise the decoration technique of the wooden ceiling of the House* of the Telephus Relief in Hercolaneum (Italy), Microchemical Journal 116, p. 7-14

[Vog1984] Vogel j S, Southon JR, Nelson, Brown T.A., *Performance of catalytically condensed carbon for use in accelerator mass spectrometry*, Nuclear Instruments and Methods B 5, p 289-293

[Wac2010] Wacker L., Nemec M., Bourquin J., *A revolutionary graphitisation system: fully automated, compact and simple*, Nuclear Instruments and Methods B 268, p 931-934

[wIa2011] http://www.iaea.org/

ACKNOWLEDGEMENTS

I am grateful to Mariaelena Fedi for her essential suggestions and support during the PhD course. Thank you to Prof. Pier Andrea Mandò for the precious possibility to work at LABEC laboratory.

I am thankful to Prof. Antonella Salvini, Department of Chemistry (University of Florence), for the fruitful discussion about the FT-IR spectra interpretation, to Luca Rosi, Department of Chemistry (University of Florence), for the artificial ageing of wooden samples and to Prof. Iacopo Moggi Cecchi, Department of Biology (University of Florence), for providing us the bone samples analysed here.